

Geology of the Martian crustal dichotomy boundary: Age, modifications, and implications for modeling efforts

Rossman P. Irwin III^{1,2} and Thomas R. Watters³

Received 24 May 2010; revised 28 July 2010; accepted 11 August 2010; published 20 November 2010.

[1] The contrast in crustal thickness, surface age, elevation, and morphology between the southern cratered highlands and northern lowland plains of Mars is termed the crustal dichotomy. The oldest exposed sections of the crustal dichotomy boundary are ancient cratered slopes, which influenced post-Noachian fresh crater morphometry, Late Noachian valley network planform, and the degradation patterns of Middle to Late Noachian (~3.92–3.7 Ga) impact craters. Noachian visible and topographically defined impact craters at the top of the cratered slope show no evidence of flexure-induced normal faulting. These observations and published geophysical data collectively require an Early to Pre-Noachian age for the crustal dichotomy, prior to the largest recognized impact basins. Late Noachian plateau deposits and more prolonged Tharsis volcanism appear to have buried parts of the old cratered slope, and fretted terrain developed in this transition zone during the Early Hesperian Epoch (~3.7–3.6 Ga). Fretted/knobby terrains, lowland plains, and most visible structures (wrinkle ridges, fractures, and normal faults) postdate Noachian crater modification and are several hundred million years younger than the cratered slope of the crustal dichotomy, so they provide no valid basis or constraint for models of its formation. Long-wavelength topography in cratered terrain dates to Early to Pre-Noachian time and provides a useful model constraint. Geological and geophysical observations are thus reconciled around an early age and relatively rapid development of the Martian crustal dichotomy.

Citation: Irwin, R. P., III, and T. R. Watters (2010), Geology of the Martian crustal dichotomy boundary: Age, modifications, and implications for modeling efforts, *J. Geophys. Res.*, 115, E11006, doi:10.1029/2010JE003658.

1. Introduction

[2] The three major geologic provinces of Mars are the Noachian (~3.7–4.5 Ga) cratered highlands, younger (<3.7 Ga) plains of the northern lowlands, and the long-lived Tharsis volcanic upland, which is centered on the transition between the highlands and lowlands [Andrews-Hanna *et al.*, 2008] (age estimates herein are based on cited geologic maps, including those of Scott *et al.* [1986–1987] and Tanaka *et al.* [2005] and the absolute chronology of Hartmann and Neukum [2001]). The highly degraded impact basins and craters of the southern highlands record an origin early in the time of heavy impact bombardment [e.g., Murray *et al.*, 1971; Schultz *et al.*, 1982; Schultz and Frey, 1990; Frey, 2006b]. The lightly cratered lowland plains are of volcanic and sedimentary origin [e.g., Carr, 1981; Lucchitta *et al.*, 1986; Bandfield *et al.*, 2000; Head *et al.*, 2002; Tanaka *et al.*, 2003, 2005], and their modal elevation is ~6 km below that of the highlands [Smith *et al.*, 2001].

These plains materials appear to superimpose older, low-lying cratered terrain based on embayment of Noachian craters around the margin, prominent islands of fractured older material [Tanaka *et al.*, 1992], and widespread quasi-circular depressions and sounding radar echoes that have been interpreted as buried impact craters [Frey *et al.*, 2002; Buczkowski *et al.*, 2005; Watters *et al.*, 2006; Frey, 2006a, 2008a; Buczkowski, 2007; Edgar and Frey, 2008]. An isostatically compensated, northward decline in crustal thickness from ~60 to 30 km facilitated resurfacing of the thin-crust lowlands and is responsible for contrasts in elevation, surface age, and morphology between the two hemispheres [e.g., Lingenfelter and Schubert, 1973; Phillips *et al.*, 1973; Zuber *et al.*, 2000; Neumann *et al.*, 2004]. These regional differences are collectively termed the crustal dichotomy.

[3] Investigators have often used geologic contacts or an escarpment to define the highland/lowland boundary, but the northward decline in crustal thickness and elevation is commonly more gradual, and much of its topographic relief occurs within cratered terrain. In Noachis Terra, most of the crustal thinning occurs well within Noachian terrain about 2500 km southeast of the lowland plains (Figure 1). Crustal thickness and topography then decline more gradually through the lowstanding, cratered Arabia Terra northward to the lowland plains [Zuber *et al.*, 2000; Neumann *et al.*, 2004].

¹Planetary Science Institute, Tucson, Arizona, USA.

²Also at Planetary Geodynamics Laboratory, NASA Goddard Space Flight Center, Greenbelt, Maryland, USA.

³Center for Earth and Planetary Studies, National Air and Space Museum, Smithsonian Institution, Washington, D.C., USA.

A cratered slope on the margin of the Amenthes, Aeolis, and Memnonia highland regions is steeper but still not abrupt (Figure 2). A single steep scarp incorporates most of the crustal dichotomy's topographic relief only in fretted terrain between 40°E and 80°E (Figure 3). For these reasons, we use the common term crustal dichotomy boundary to describe the major decline in crustal thickness and topography that occurs primarily within cratered terrain (described in section 2.1), and plains/upland contact refers to the southern margin of the lowland plains. The transition zone (described in section 2.2) includes fretted/knobby terrains and the younger plateau units in which they formed, located between heavily cratered terrain and the plains/upland contact over part of the circumference of Mars (specifically ~10°E–80°E and 120°E–155°E). The transition zone locally includes a boundary scarp that is 1–2 km high and near the angle of repose (Figure 3).

[4] The cause of the crustal dichotomy has remained a major issue in our understanding of Mars [e.g., Nimmo and Tanaka, 2005; Watters *et al.*, 2007] since its discovery [McCauley *et al.*, 1972]. Most qualitative and quantitative geophysical models have invoked long-wavelength mantle convection and regional crustal thinning during or after the planet's interior differentiation [Lingenfelter and Schubert, 1973; Wise *et al.*, 1979; Davies and Arvidson, 1981; McGill and Dimitriou, 1990; Zhong and Zuber, 2001; Roberts and Zhong, 2006], but some investigators have favored plate tectonics [Sleep, 1994; Lenardic *et al.*, 2004] or one or more large/giant impacts in the Northern Hemisphere as causal mechanisms [Wilhelms and Squyres, 1984; Frey and Schultz, 1988, 1990; Frey, 2006a, 2006b; Andrews-Hanna *et al.*, 2008; Marinova *et al.*, 2008; Nimmo *et al.*, 2008]. Most of the earlier critical reviews concluded that an endogenic process is probably needed to explain the hemispheric scale differences in crustal thickness but that some early large impacts are also evident [McGill and Squyres, 1991; Zuber, 2001; Nimmo and Tanaka, 2005; Solomon *et al.*, 2005]. Other studies have focused on modifications to the crustal dichotomy boundary, which have been attributed to various erosional processes [e.g., Sharp, 1973; Sharp and Malin, 1975; Guest *et al.*, 1977; Scott, 1978; Soderblom and Wenner, 1978; Squyres, 1978, 1979; Breed *et al.*, 1982; Lucchitta, 1984; Kochel and Peake, 1984; Manent and El-Baz, 1986; Dimitriou, 1990; Carr, 1995, 2001; Carruthers and McGill, 1998; Mangold, 2003; Irwin *et al.*, 2004; Chuang and Crown, 2005; Head *et al.*, 2006; Levy *et al.*, 2007], disruption of highland terrain by extensional faulting [Mutch *et al.*, 1976, pp. 232–234; McGill and Dimitriou, 1990; Smrekar *et al.*, 2004; Guest and Smrekar, 2005], relaxation due to lateral crustal flow [Nimmo and Stevenson, 2000; Nimmo, 2005], and flexure of the elastic lithosphere by loading of the lowlands [Watters, 2003a, 2003b; Watters and McGovern, 2006].

[5] The first 300–500 Myr of Martian history are difficult to interpret uniquely, because heavy impact bombardment saturated the planet during that time. Nonetheless, several lines of evidence, including isotopic analysis of Martian meteorites [Chen and Wasserburg, 1986; Harper *et al.*, 1995; Borg *et al.*, 1997; Blichert-Toft *et al.*, 1999; Halliday *et al.*, 2001; Marty and Marti, 2002], the 4.5 Ga age of meteorite ALH 84001 [Nyquist *et al.*, 2001], and analogy to Pre-Nectarian crustal development of the Moon [e.g., Warren, 1985; Wilhelms, 1988], consistently suggest that most of the solid crust developed by ~4.5 Ga, within the first ~50 Myr after planetary accretion [Solomon *et al.*, 2005; Nimmo and Tanaka, 2005]. Adequate heat from accretion, decay of short-lived radioisotopes, and core formation was available to melt the planet, and a magma ocean appears required for interior differentiation [Elkins-Tanton *et al.*, 2005; Jacobsen, 2005; Terasaki *et al.*, 2005]. The crustal dichotomy is isotopically well compensated relative to the largest impact basins and the major regions of later Noachian and Hesperian volcanic resurfacing [Phillips and Saunders, 1975; Janle, 1983; Smith *et al.*, 1999; Zuber *et al.*, 2000], suggesting that the dichotomy formed during a time of high internal heat flow. The strong magnetic signature of much of the southern highland crust records an early geomagnetic field, which also appears to have declined during the Pre-Noachian Period (defined by Tanaka *et al.* [2005] as time before the relict cratering record was established; the Early Noachian Epoch defined by Tanaka [1986] includes the Pre-Noachian Period). Impact processes and heating permanently demagnetized areas near the major highland basins around 4.1 Ga, and younger volcanic rocks were not magnetized [Acuña *et al.*, 1999; Connerney *et al.*, 1999, 2005; Frey, 2006b, 2008a; Lillis *et al.*, 2008]. The magnetic signature is also present but relatively weak over the northern lowlands, outside the nonmagnetic Utopia and polar basins [Connerney *et al.*, 1999, 2005]. This occurrence suggests that the crustal dichotomy formed while the magnetic field was still active or at least declining, consistent with the Early Noachian minimum age of lowland crust inferred from populations of quasi-circular depressions, interpreted as buried impact craters [Frey *et al.*, 2002; Buczkowski *et al.*, 2005; Frey, 2006a, 2006b; Edgar and Frey, 2008]. Frey [2006b] also suggested that the highland crust has been stable since at least ~4.14–4.33 Ga, based on the population of large, highly degraded and/or buried, circular basins in the highlands, although a younger age would pertain if large impact basins represent a Martian equivalent of a terminal lunar cataclysm [Frey, 2008a].

[6] Considering the evidence above, Solomon *et al.* [2005] suggested that the crustal dichotomy may have formed “by spatially heterogeneous fractionation of an early magma ocean” around 4.5 Ga and attributed the lowland crustal

Figure 1. Large impact basins have flat floors along the cratered slope of the crustal dichotomy boundary near 0° longitude, showing that no significant tilting occurred after the floor deposits were emplaced. (a) Low-gradient cratered slope of the crustal dichotomy boundary in Noachis Terra, bounded by 0°S, 35°S, 20°W, and 15°E; 2075 km across at the equator. Thermal Emission Imaging System (THEMIS) daytime infrared (DIR) mosaic 2.0 with missing data filled by the Viking Mars Digital Image Mosaic (MDIM) 2.1 and colorized with Mars Orbiter Laser Altimeter (MOLA) topography from the 128 pixel/degree Mission Experiment Gridded Data Record (MEGDR). Black lines are contours with a 1 km interval, and the white box is the outline of Figure 1b. (b) MOLA contour map, 100 m interval, of a subset of Figure 1a. All color figures in this paper have the same topographic color scale, and all figures have north at the top.

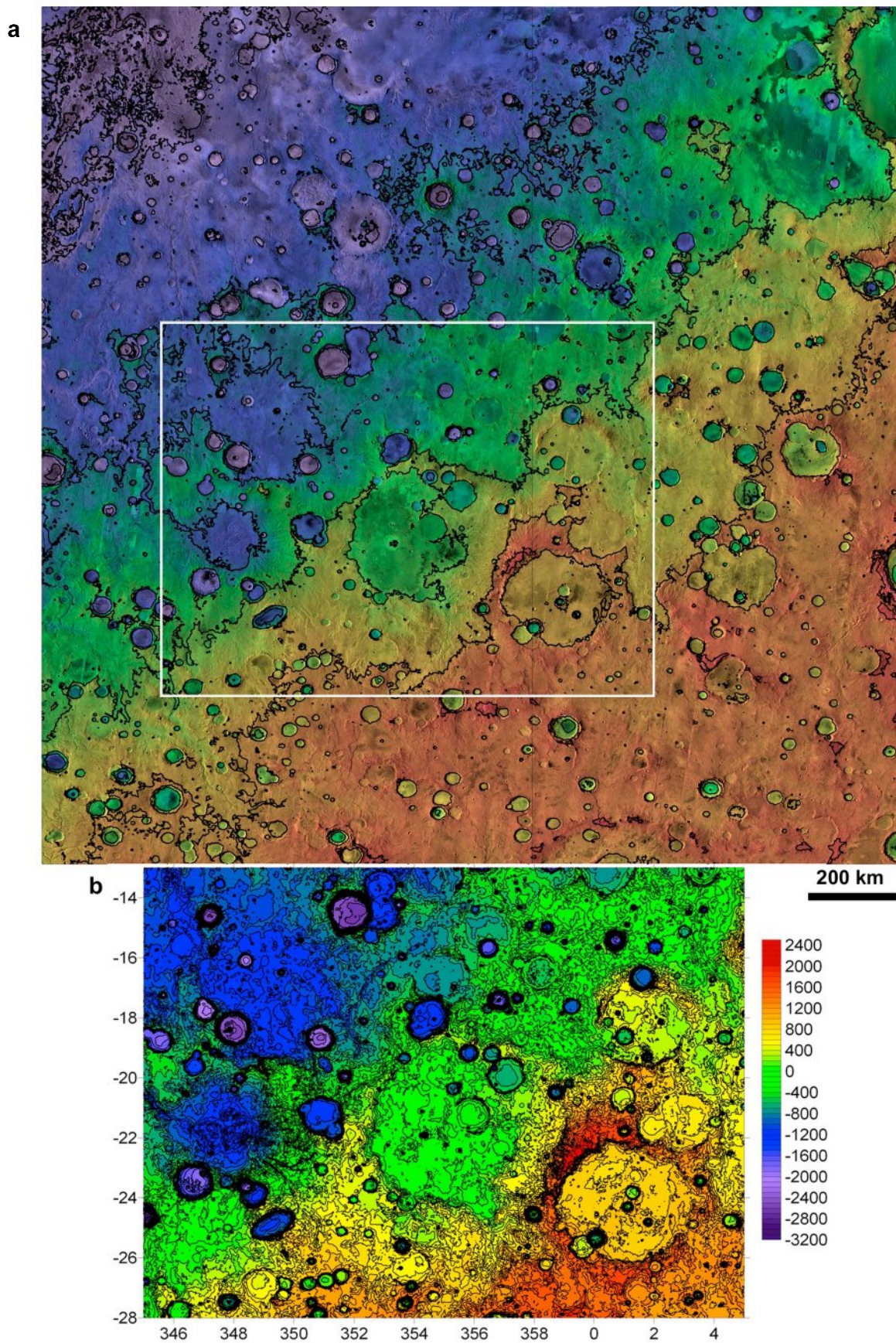


Figure 1

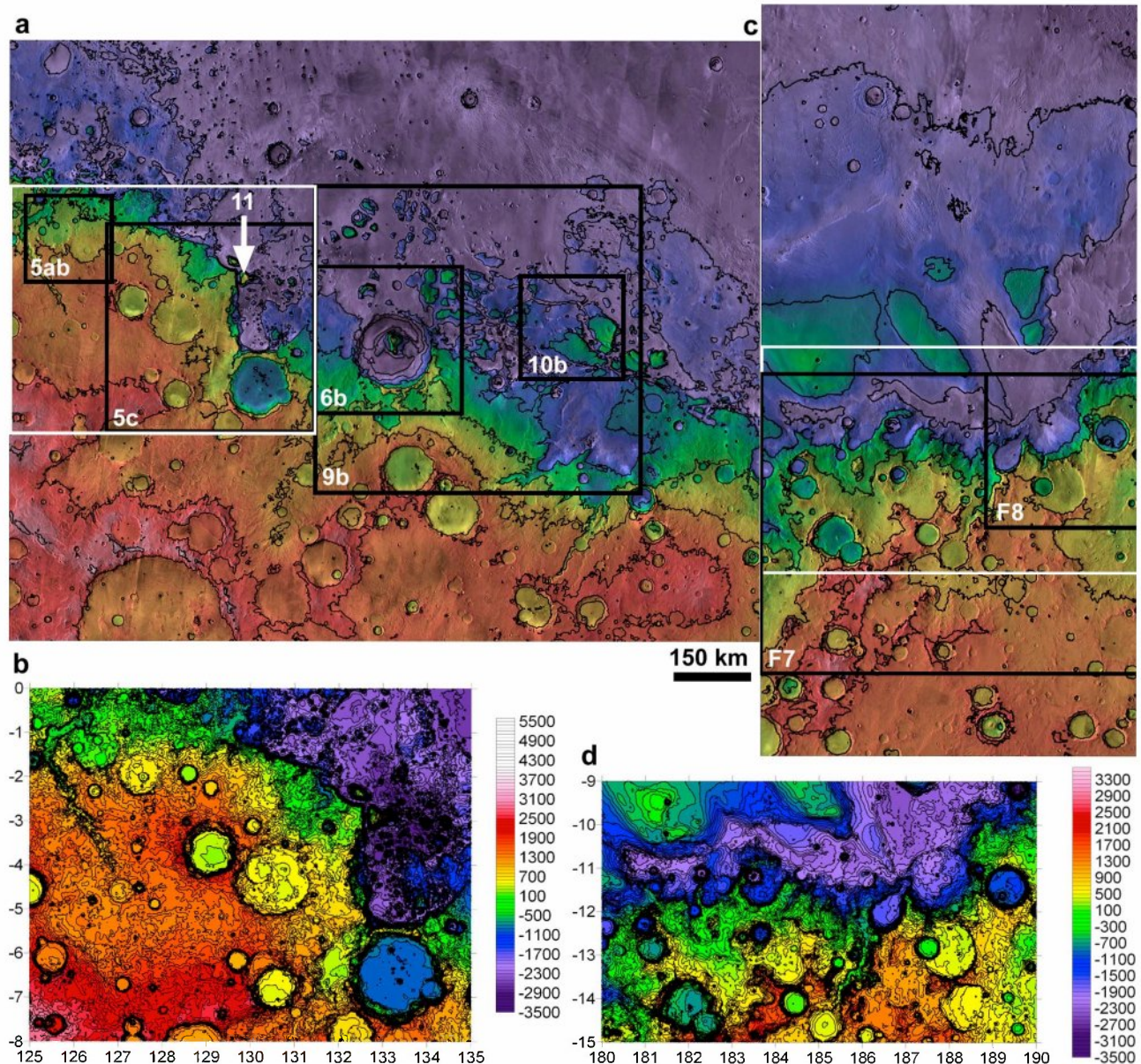


Figure 2. Degraded impact craters have flat floors along the cratered slope of the crustal dichotomy boundary near 180° longitude, showing that no significant tilting occurred after the floor deposits were emplaced. (a) Cratered slope of the crustal dichotomy boundary in Terra Cimmeria; bounded by 5°N, 15°S, 125°E, and 140°E; 889 km across at the equator. The white outline is of Figure 2b, and contour lines have a 1 km interval. (b) MOLA contour map with 100 m interval of a subset of Figure 2a. (c) Steep cratered slope of the crustal dichotomy boundary in Terra Sirenum; bounded by 0°N, 20°S, 180°W, and 175°W; 296 km across at the equator. Contour lines have a 1 km interval, and the white outline is of Figure 2d. (d) MOLA contour map with 100 m interval of a subset of Figure 2c. Both Figures 2a and 2c were prepared similarly to Figure 1a. Black outlines represent the locations of later figures.

demagnetization to regional hydrothermal alteration, having found volcanic burial or heating inadequate to remove or obscure the magnetic signature. *Nimmo and Stevenson [2000]* suggested that early degree-1 mantle overturn may have enhanced a thermal gradient at the core/mantle boundary that could have driven the core dynamo, although a hot core could have the same effect [*Nimmo and Tanaka, 2005*]. Alternatively, *Frey [2006a]* placed the origin of the lowland crust after the termination of the dynamo and closer in age to the Utopia

basin impact, which the superimposed, buried crater population constrains in age to >4.1–4.2 Ga. Long-lived plate tectonic models [*Sleep, 1994; Lenardic et al., 2004*] and some endogenic scenarios linking Hesperian fretted terrain to the origin of the crustal dichotomy boundary [*McGill and Dimitriou, 1990; Robinson, 1995; Smrekar et al., 2004; Guest and Smrekar, 2005*] have suggested much younger ages around the Noachian/Hesperian transition. The observations cited above collectively limit large/giant impacts or dichotomy-forming

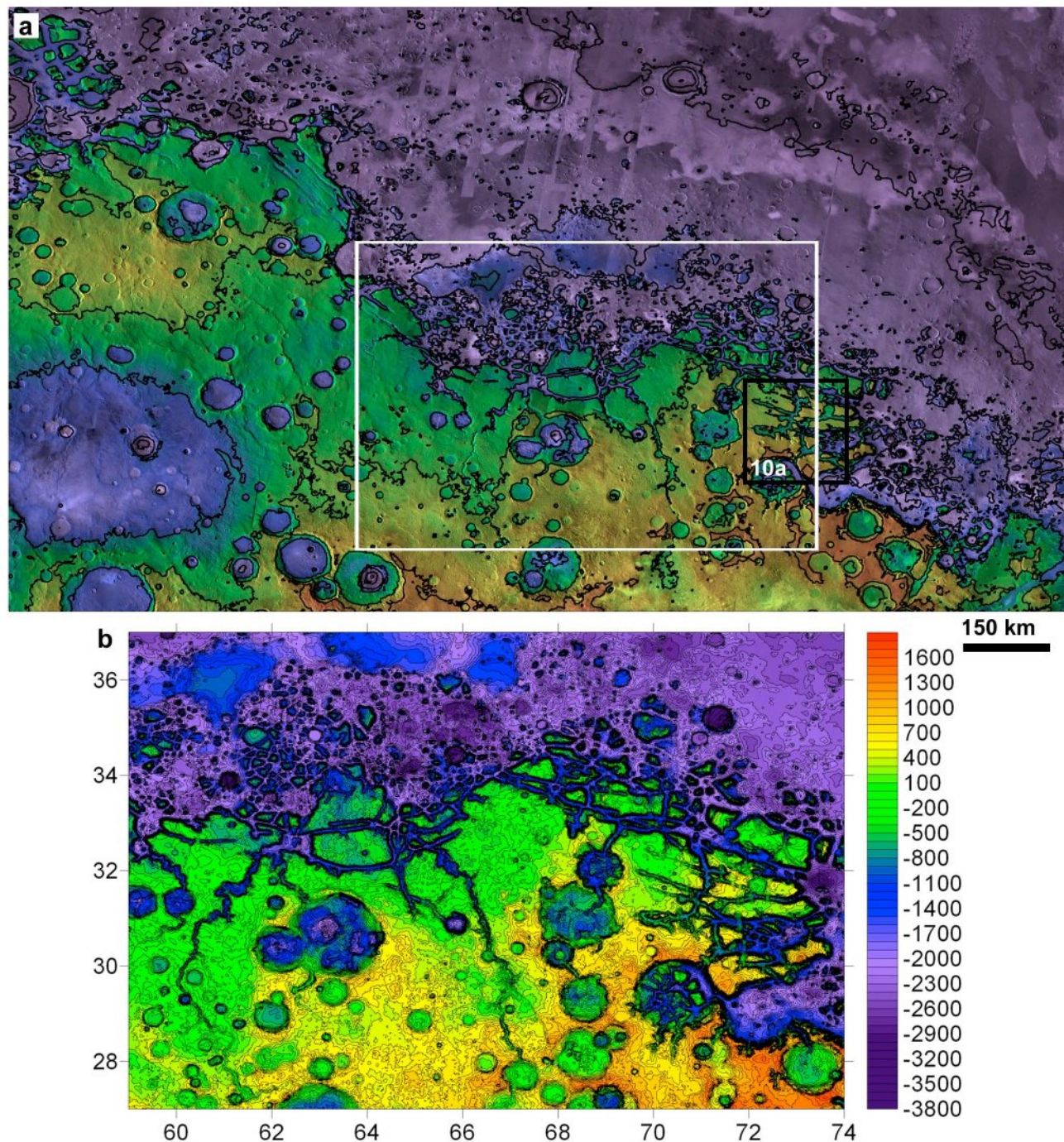


Figure 3. Steep boundary scarp at the margin of cratered terrain that otherwise slopes very gradually to the north, in contrast to cratered slopes in Figures 1 and 2. (a) Fretted and knobby terrains along the crustal dichotomy boundary in Arabia Terra; bounded by 45°N, 25°N, 45°E, and 80°E; 1880 km across at the bottom. Prepared as in Figure 1a. Black outline is the location of Figure 10a, and white outline is Figure 3b. (b) MOLA contour map with 100 m interval of a subset of Figure 3a.

endogenic processes to the earliest few tens to hundreds of millions of years of Martian history, a time that is poorly represented by surface features. Moreover, we argue below that geologic observations that have been cited in favor of a younger crustal dichotomy are equivocal or have been misinterpreted.

[7] Over the last several years, planetary literature has converged toward the idea that the crustal dichotomy is the oldest or one of the oldest features of Mars (see reviews by *Solomon et al.* [2005], *Nimmo and Tanaka* [2005], and *Watters et al.* [2007]). The purpose of this paper is to reexamine geological observations that suggested a later age

around the Noachian/Hesperian transition in order to determine whether the geology supports the findings of geophysical studies cited above and to provide some constraints on future modeling efforts. Our approach is to (1) establish disparate ages of the crustal dichotomy, Noachian crater degradation, and fretted terrain; (2) evaluate the tectonic and geomorphic evolution of the transition zone; and (3) compare our observations to existing models.

2. Geological Constraints and Interpretation

2.1. Cratered/Dissected Terrain

[8] Relationships between the long-wavelength topography and smaller landforms (impact craters and valley networks) along the crustal dichotomy boundary provide useful constraints on its age, origin, and later modification processes. Here we use landform morphology to test alternative hypotheses of (1) a primordial (contemporary formation of both the thick highland crust and the thin lowland crust) or intermediate age (hemispheric thickening and/or thinning of an initially uniform crust before the relict impact basins formed) for the crustal dichotomy within the Pre-Noachian Period, or (2) a later origin around the Noachian/Hesperian transition (thinning the lowland crust and leaving the older highland crust intact). Because of their younger age, relict landforms are not useful for differentiating ages within the first hypothesis. Superimposed impact craters are an ideal baseline landform for geomorphic studies due to their predictable initial morphometry and use in age determination [Sharp, 1968; McGill and Wise, 1972; Arvidson, 1974; Neukum and Hiller, 1981; Craddock and Maxwell, 1990, 1993; Grant and Schultz, 1990, 1993; Jankowski and Squyres, 1992, 1993; Barlow, 1995; Craddock et al., 1997; Grant et al., 1997, 2006; Forsberg-Taylor et al., 2004; Howard, 2007]. Local precrater topography influenced both the primary morphology and degradation patterns of impact craters [e.g., Irwin and Howard, 2002; Forsberg-Taylor et al., 2004; Irwin et al., 2005], as well as the planform of valley networks [e.g., Pieri, 1980; Grant, 1987; Irwin and Howard, 2002]. The change in impact crater geometry with advancing degradation [Arvidson, 1974; Craddock and Maxwell, 1990, 1993; Craddock et al., 1997; Craddock and Howard, 2002; Forsberg-Taylor et al., 2004] and differences in this pattern with a crater's topographic setting [Irwin and Howard, 2002] are well defined, so it is straightforward to determine whether tectonic tilting, compression, or extension modified impact craters during their degradation. The diverse states of modification (degradation of the ejecta, crater rim, interior wall terraces, and central peak, with associated infilling) among many adjacent impact craters of similar diameter and the often advanced degradation of large craters relative to smaller ones that should have been infilled more rapidly show that fluvial erosion was prolonged and ubiquitous throughout at least the Middle and Late Noachian Epochs [e.g., Craddock and Maxwell, 1993].

[9] Our tests of existing hypotheses focus on the northward-sloping cratered terrain found in both the Arabia (gentler slope) and Cimmeria/Sirenum (steeper slope) broad embayments in the crustal dichotomy boundary (Figures 1, 2a, and 2b). If the highland crust had been flexed and tilted northward after the visible craters formed (the late origin hypothesis), then grabens near the upper break in slope and

compressional ridges lower on the slope should crosscut the craters, with faults generally striking parallel to the boundary [Watters, 2003a, 2003b]. Tilting would have altered fluvial transport pathways, resulting in partial erosion of older deposits and (depending on the relative timing of lowland formation) a divergence of Late Noachian valley networks from local topographic gradients. Alternatively, if the slope predates the visible degraded craters (the Early to Pre-Noachian origin hypotheses), then it should have affected their morphology and controlled the planform of valley networks.

[10] Our understanding of fluvial crater degradation is based on theoretical modeling and empirical studies on Earth and Mars [Craddock and Maxwell, 1993; Grant and Schultz, 1993; Grant et al., 1997; Craddock et al., 1997; Craddock and Howard, 2002; Forsberg-Taylor et al., 2004; Howard, 2007]. A fresh complex crater has a central peak or peak ring, terraced or hummocky interior walls, a raised rim, and a rugged ejecta blanket. Fluvial erosion of the steep interior wall incises gullies, removes terraces, and widens the crater at the expense of its rim. The resulting debris partly fills the interior cavity and buries the eroded central peak, producing a relatively flat floor deposit. Over time, infilling and rim erosion reduce the interior relief and with it the rate of widening. Outside the rim, the texture of the ejecta blanket is lost early, but erosion is slow due to the lower gradient, high permeability, and a radial-centrifugal drainage pattern [Pieri, 1980] that disperses rather than concentrates overland flow. The resulting basin is sometimes called the "cookie-cutter" morphology (Figures 4a and 4c). The low relief of the broader ejecta blanket may isolate the basin from exterior sediment supplies for some time. Breaching of impact craters on flat plains requires prolonged erosion of the rim and ejecta, aggradation of the exterior surface, or flooding of a basin outside the reduced crater rim. Craters rapidly fill with sediment once they are breached. Many small impact craters are lost while the larger ones are degraded due to their lower rim relief and higher ratio of erosional wall area to volume [e.g., Neukum and Hiller, 1981; Strom et al., 1992; Forsberg-Taylor et al., 2004].

[11] For impact craters emplaced on older slopes, the plane defined by the crater rim generally inclines subparallel to the exterior slope, whereas the interior cavity is oriented vertically [Irwin et al., 2005] (Figures 4b and 4d). The relief of the upslope interior wall is greater than that of the downslope equivalent, encouraging more rapid backwasting of the former, while sediment is transported toward the upslope rim from higher surfaces. For these reasons, breaching of the upslope rim and infilling occurs more rapidly on precursor slopes [Irwin and Howard, 2002; Howard, 2007]. Throughout this time, the floor deposit accumulates with a flat to slightly concave topographic profile (Figure 4c). The late-stage form resembles an amphitheater, with water from the contributing slope flowing over the upslope wall, through the crater, and out across its buried downslope rim (Figures 5a and 5b). Impact craters with deeply dissected ejecta blankets are often larger and/or located on precursor ridges or slopes, making the ejecta steeper than it would otherwise be in the latter case [Irwin and Howard, 2002].

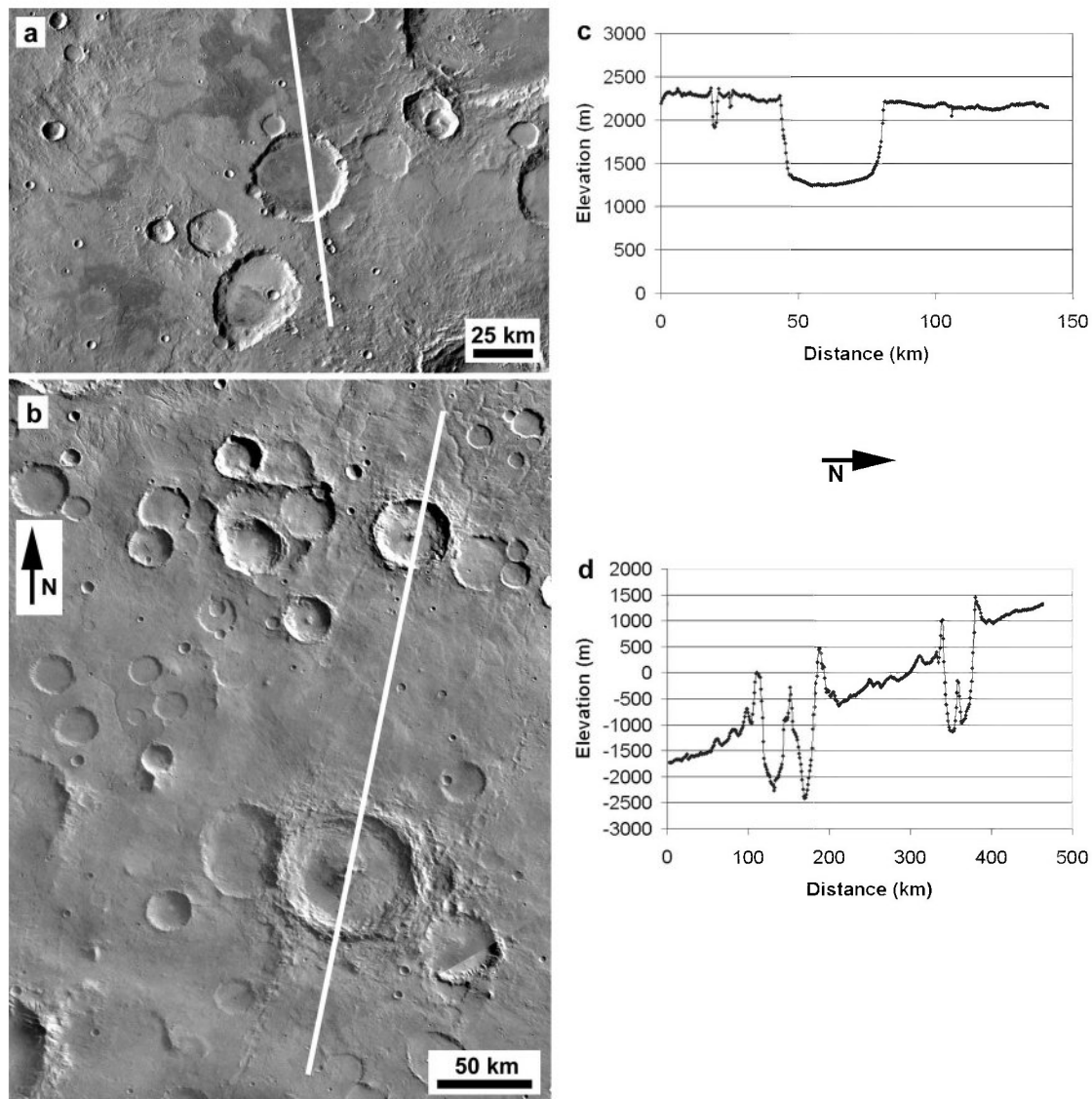


Figure 4. (a) A degraded Noachian impact crater on a flat surface. The crater displays the “cookie-cutter” morphology, in contrast with degraded craters on a precrafter slope shown in Figure 5. The white line is the surface track of the topographic profile in Figure 4c. THEMIS DIR mosaic 2.0 centered at 25.4°S, 131.6°E. (b) Two fresh impact craters on the northern slope of the Hellas basin, adapted from *Irwin et al.* [2005]. The white line is the topographic profile shown in Figure 4d. Viking MDIM 2.1 centered at 25.6°S, 87.4°E. (c) MOLA shot data crossing the degraded crater in Figure 4a. (d) Topographic profile of the craters in Figure 4b from gridded MOLA MEGDR data, 64 pixels/degree. Note the vertical orientation of the interior cavity and the rim crests that are roughly parallel to the exterior surface.

[12] These relationships are useful for interpreting the heavily cratered slopes associated with declines in crustal thickness [*Neumann et al.*, 2004]. From about 105°E to 215°E, the northward decline in elevation is relatively steep (~ 0.5 – 1.5°) and occurs within Early to Middle Noachian cratered terrain [*Frey et al.*, 1998]. This slope is best exposed in the Aeolis and Memnonia quadrangles in Terra Cimmeria and Terra Sirenum, respectively, where fretted/chaotic terrains and Medusae Fossae deposits cover only its lower-lying areas (Figures 2c and 2d). The heavily cratered crust thins more gradually ($\sim 0.1^\circ$ in Noachis Terra, Figure 1) to the north in the Xanthe, Margaritifer, Noachis, and Arabia

Terrae regions (305°E eastward to 40°E) [*Zuber et al.*, 2000; *Neumann et al.*, 2004]. The occurrence of an ancient cratered slope is less certain where Tharsis volcanic rocks bury the boundary (215°E–305°E) and where Protonilus and Nilosyrtris Mensae fretted terrain (40°E–90°E) formed in the highstanding plateau (Figure 3), but its occurrence between these two regions suggests that the cratered slope was originally continuous. A recent analysis of isostatic crustal root thickness suggested that the Noachian Tharsis load is roughly centered on an older dichotomy boundary [*Andrews-Hanna et al.*, 2008].

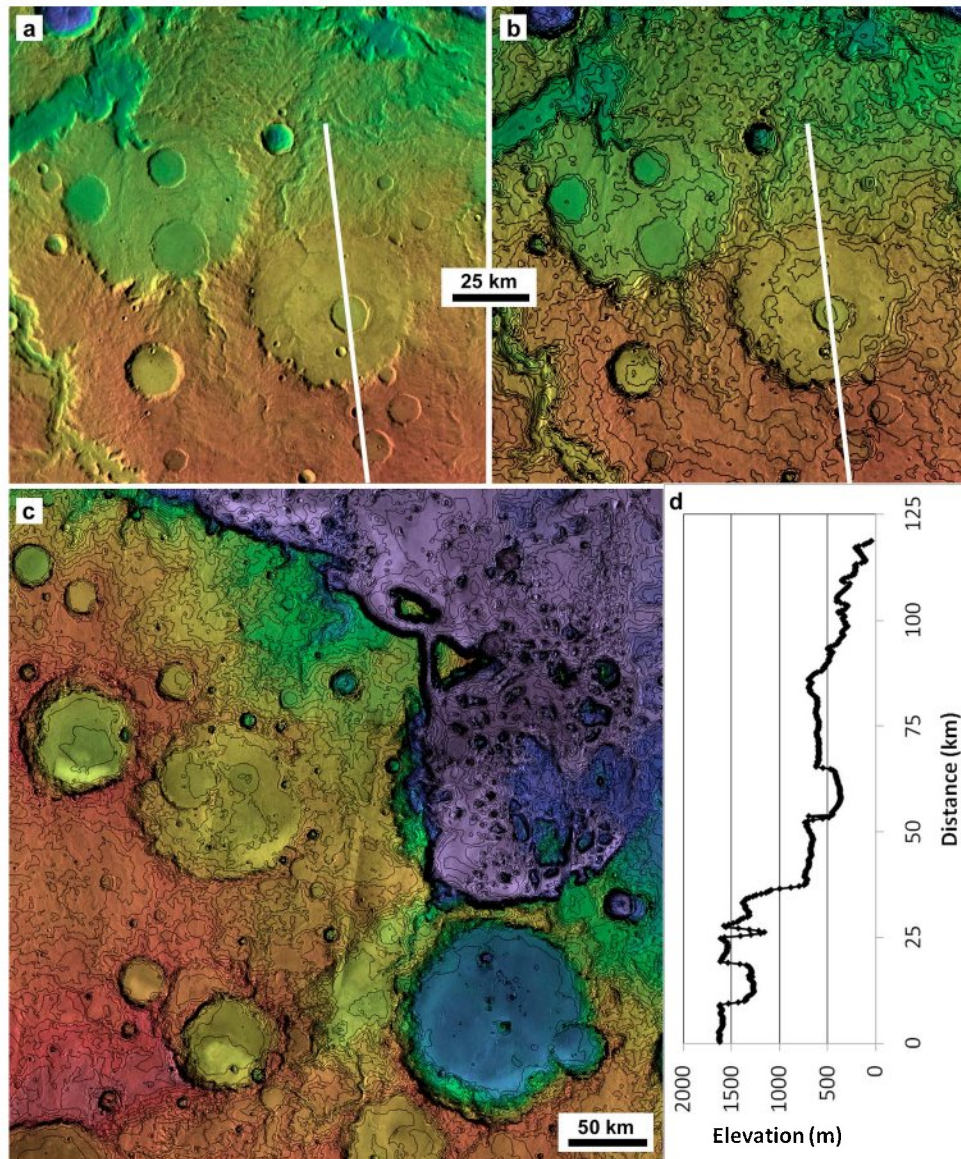


Figure 5. (a, b) Highly degraded Noachian impact craters with smaller degraded craters on their flat floors. The large craters have the amphitheater morphology, reflecting degradation on a precrater slope, whereas the smaller craters on their floors have the cookie cutter morphology, reflecting degradation on a flat surface. The larger craters were not tilted after the small craters formed in the later part of the Noachian Period. Image centered at 1.5°S, 127°E. (c) A similar scene to the east, centered at 4.3°S, 131.7°E, showing flat-floored craters next to the very abrupt boundary scarp. Image data as in Figure 1a with a 50 m contour interval in Figures 5b and 5c. (d) Topographic profile of an amphitheater-shaped degraded crater and a smaller degraded crater superimposed on its floor. MOLA shot data with location indicated by the white line in Figures 5a and 5b.

[13] The heavily cratered slope influenced post-Noachian fresh crater morphometry, Late Noachian valley network planform, and the degradation patterns of Middle to Late Noachian impact craters and drainage basins, requiring an earlier origin of the crustal dichotomy. Counts of fresh-appearing impact craters >5 km diameter along the cratered slope establish that crater modification rates declined severely around the Noachian/Hesperian transition [e.g., Maxwell and McGill, 1988; Craddock and Maxwell, 1990, 1993; Irwin and Howard, 2002; Golombek et al., 2006], so the superimposed fresh craters are this age and younger.

Fresh and slightly modified (post-Noachian) craters in Noachian geologic units along the dichotomy boundary have rim planes that incline subparallel to the slope (Figure 6), but the lack of extensional faulting high on the cratered slope (Figures 1, 2, 5, and 6) establishes that no large-scale lithospheric flexure occurred during or after the Early Hesperian.

[14] Although slow fluvial erosion of the highlands was long-lived, the incised valley networks and well-preserved alluvial deposits are primarily Late Noachian to Early Hesperian in age (they each postdate the youngest degraded craters in their vicinity), and many of them could have

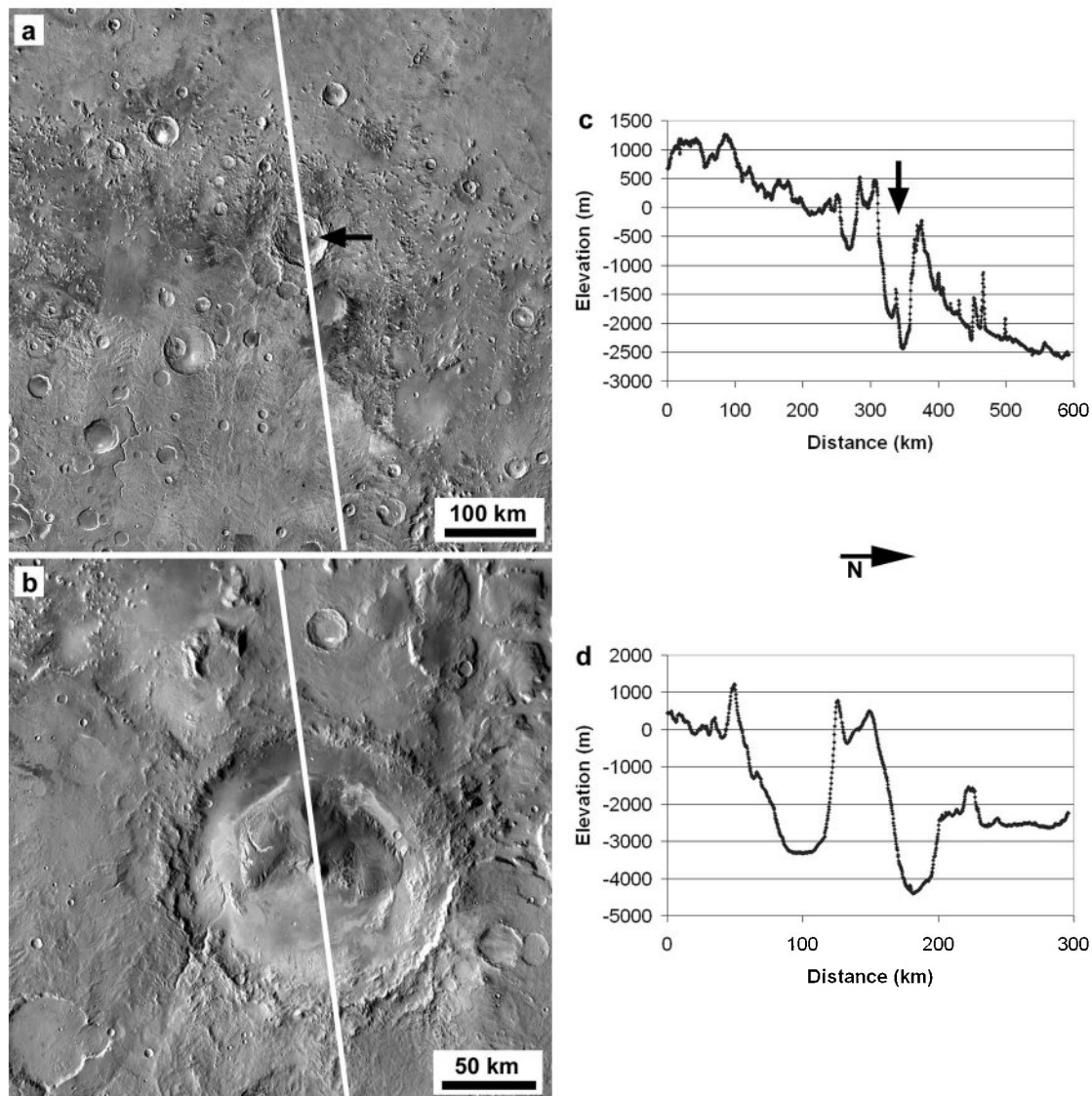


Figure 6. Fresh and somewhat degraded craters on the cratered slope of the crustal dichotomy boundary. In both cases the rim crest is inclined parallel to the exterior slope, whereas the interior cavity is oriented vertically, consistent with an impact on an older slope. (a) A fresh crater at 8°N, 119°E, indicated by the black arrow. The white line is the MOLA shot track shown in Figure 6c. (b) Gale crater (5°S, 138°E), which was deeply buried and partly exhumed, mostly by wind, after its emplacement around the Noachian/Hesperian transition. The white line is the MOLA shot track shown in Figure 6d.

formed in less than a million years in an Earthlike arid to semiarid climate [e.g., Dohrenwend *et al.*, 1987; Bhattacharya *et al.*, 2005]. Higher-magnitude runoff that incised valleys, as contrasted with more ubiquitous fluvial erosion of lower intensity, may have been episodic and appears to have peaked around the Noachian/Hesperian transition [Howard *et al.*, 2005; Irwin *et al.*, 2005]. For these reasons, valley networks may constrain the crustal dichotomy to the Late Noachian Epoch or earlier, but they are not useful in establishing what earlier age may pertain. We derived overland flow paths using Rivix RiverTools 3.0 software and the 128 pixel/degree Mars Orbiter Laser Altimeter (MOLA) grid, and these predictions matched observations of small valleys in Mars Odyssey Thermal Emission Imaging System (THEMIS) 256 pixel/degree

mosaics of the cratered slope (Figure 7). Late Noachian tributary valleys converge down modern intercrater slopes, and overflowing streams incised the original low points of basin divides, so the cratered slope predates and controlled at least the later stages of fluvial erosion in the area. Valleys oriented east/west would diverge from the local slope if the surface had been tilted northward after they became inactive, but we find no difference between the courses of these valleys and their local maximum topographic gradients (Figure 7). The muted topography of older Noachian impact basins, slopes associated with the crustal dichotomy, and other broad uplands of undetermined origin dominate the cratered (Npl₁) and dissected (Npl_d) units of Scott *et al.* [1986–1987] at 100–1000 km length scales [e.g., Grant, 1987; Irwin and Howard, 2002; Frey, 2006a, 2006b].

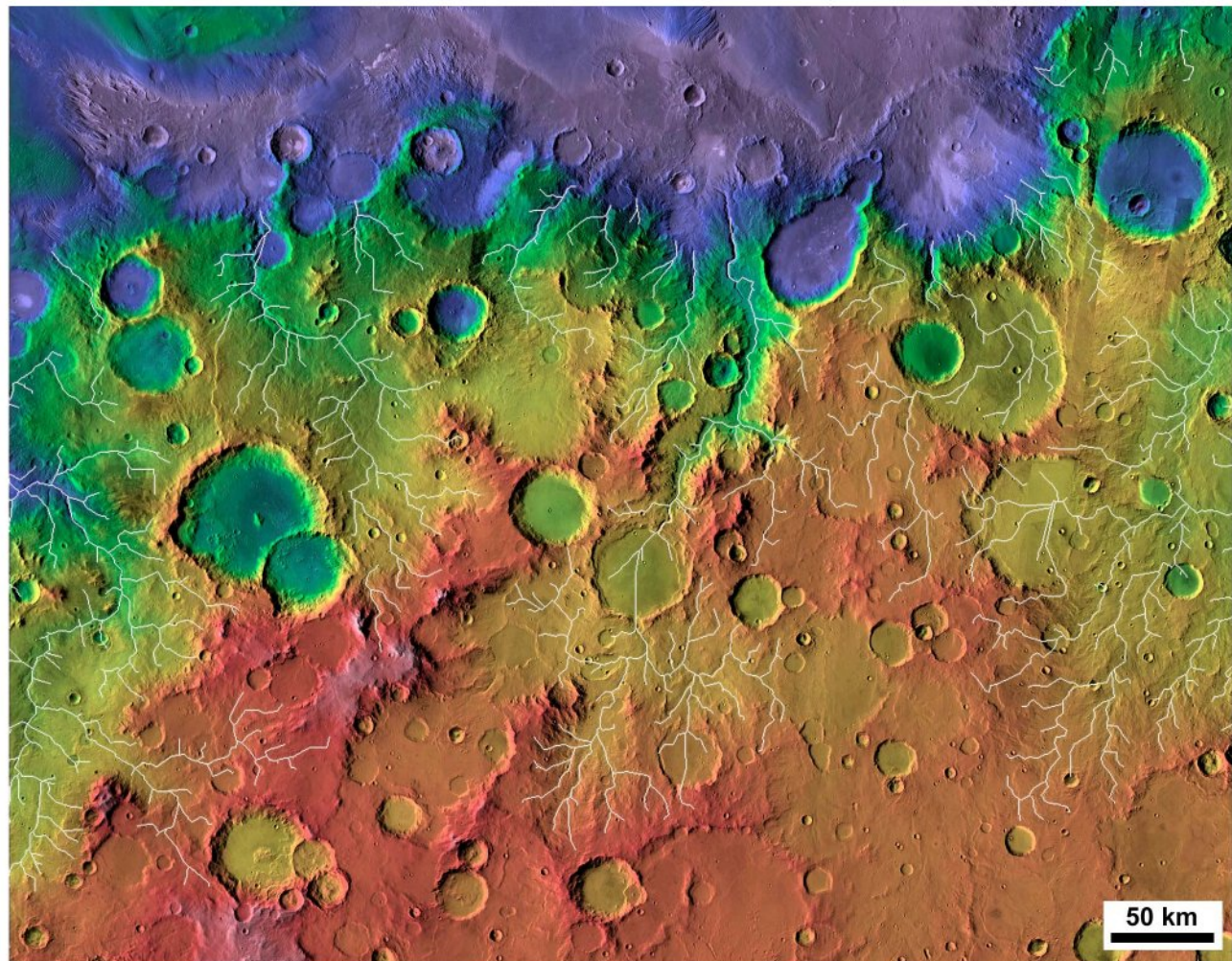


Figure 7. Computationally derived flow paths for surface water down the crustal dichotomy slope closely match the actual locations of valley networks, demonstrating that no significant tilting of the dichotomy boundary occurred after the valleys formed in the Late Noachian Epoch. Base image prepared as in Figure 1a. The white lines are not intended to reflect the drainage system fully or precisely at all locations but to demonstrate that modern topography controlled ancient flows of surface water, as found by *Phillips et al.* [2001]. Large areas within the scene that did not drain across the crustal dichotomy boundary are cleared of derived stream paths. Image bounded by 180°E, 190°E, 10°S, and 17.8°S.

Global flexure associated with Tharsis loading either pre-dates the valley networks [*Phillips et al.*, 2001] or only negligibly altered the topography after they formed.

[15] As the relict valley networks were incised late in the Noachian Period, we examined degraded impact craters and intercrater surfaces for any earlier geomorphic response to tilting. Noachian craters within the northward sloping cratered and dissected units [*Scott et al.*, 1986–1987] have floors that are flat or slightly concave rather than north-sloping (Figures 1, 2, and 8), so tilting can not have occurred after the floor deposits were emplaced up to around the Noachian/Hesperian transition. If previously flat crater floors had been tilted and then reworked during the Late Noachian Epoch, then the southern half of the crater floor would initially become dissected, but we have found no evidence of such reworking. In the older crater amphitheaters shown in Figure 5, the flat floors contain smaller cookie-cutter craters, which reflect prolonged degradation on that

locally flat surface. These larger craters have not been tilted since the smaller interior craters were superimposed and eroded in the later part of the Noachian Period. The few craters that do have dissected floors are interspersed with flat-floored craters along the steepest cratered slopes (Figure 8); erosional lowering of crater rims or infilling provided an outlet for surface water, allowing floor dissection in these few cases. We also find no intercrater basin deposits that appear to have been tilted and dissected. These observations constrain the development of a cratered slope along the crustal dichotomy boundary to the Middle to Early Noachian Epochs or the Pre-Noachian Period.

[16] Visible impact craters and valley networks do not constrain when the dichotomy formed during this ~600–700 Myr interval of time, but they do show that the high-relief slopes along the margins of cratered terrain, and thus the crustal dichotomy, significantly predate the Early Hesperian fretted and knobby terrains of the transition zone. In

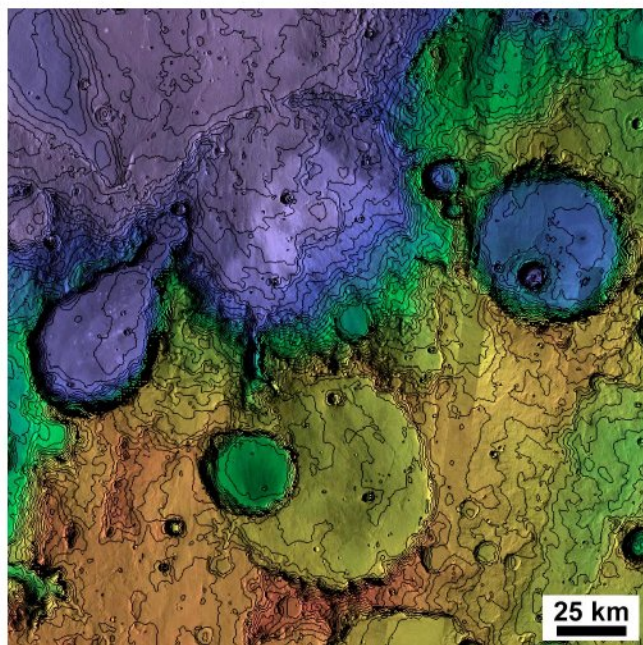


Figure 8. Flat-floored craters along the crustal dichotomy boundary slope and a more heavily degraded crater that has an eroded floor (top, center). No tilting occurred after the flat-floored craters were emplaced, and the erosion of the one crater's floor is due to prolonged erosion of the rim, which provided an outlet for surface water. Base image prepared as in Figure 1a with 100 m contour interval, centered at 12°S, 188°E.

contrast, the highlands around the Hellas and Isidis basins contain prominent extensional structures, most of which are attributed to mascon loading in the Middle to Late Noachian Epochs [Solomon and Head, 1980; Wichman and Schultz, 1989]. Models of lowland subsidence, volcanic loading, or lateral crustal flow and extension along the crustal dichotomy boundary also predict extension on the cratered slope [e.g., McGill and Dimitriou, 1990; Watters, 2003a, 2003b; Guest and Smrekar, 2005; Nimmo, 2005]. The absence of extensional structures on the cratered slope or in the highlands suggests that the crustal dichotomy predates the entirety of the visible and MOLA-defined cratering record (i.e., that it is Early to Pre-Noachian in age). No topographic features on Mars have been uniquely interpreted to predate the crustal dichotomy boundary in cratered terrain.

2.2. Transition Zone (Fretted and Knobby Terrains)

[17] The observations above demonstrate a long temporal break between the Early to Pre-Noachian origin of the crustal dichotomy and development of Early Hesperian features within the transition zone. In this context it is useful to examine alternative explanations for fretted and knobby terrains, given their association with some high-relief sections of the crustal dichotomy boundary, evident structural control, and use in prior literature as evidence for specific geophysical processes related to the dichotomy [e.g., Mutch et al., 1976; McGill and Dimitriou, 1990; Smrekar et al., 2004; Nimmo, 2005]. Our purpose here is not to derive a complete explanation for fretted terrain but to summarize what is known and unknown about it and the relevance of

these points to investigations of the crustal dichotomy. A central issue in interpreting the transition zone is the relative roles of structural and geomorphic processes, both of which appear to have been important.

2.2.1. Description of the Transition Zone

[18] In contrast to the erosion and infilling of coherent impact craters in the Noachian highlands, highstanding surfaces have been severely disrupted in the transition zone, leaving mesas and rounded knobs (“mensae” and “colles”, respectively) that extend for hundreds to over a thousand kilometers into the lowlands (Figure 3). Sharp [1973] defined fretted terrain as “characterized by smooth, flat, lowland areas separated from a cratered upland by abrupt escarpments of complex planimetric configuration and a maximum estimated height approaching 1–2 km.” The relatively flat (at least at low resolution) lowland areas and lack of large slump blocks distinguish fretted terrain from chaotic terrain, which has jumbled floors of angular blocks and evidence of wall failure [Sharp, 1973]. Sharp and Malin [1975] defined “fretted channels” as “steep-walled features with wide, smooth, concordant floors. Planimetric configuration can be complex, with irregularly indented walls, integrated craters, and control by linear crustal structures, presumably fractures, often evident. Isolated butte- or mesa-like structures are common, and extensive lateral integration of adjacent channels has occurred locally.”

[19] Fretted valleys can be divided on the basis of morphology into two general classes, which may have different origins. Some of them are sinuous, oriented along the steepest local gradients, and in possession of stubby tributaries, all consistent with a fluvial origin [e.g., McGill, 2000; Carr, 2001]. A far greater number are straight or arcuate in plan view, and they intersect in an irregular gridded pattern (Figure 3). In contrast to valley networks, which are (with very few exceptions) oriented down the steepest local gradients, the latter class of fretted valleys appears mostly independent of topographic control (Figure 9) and often lacks continuously declining longitudinal profiles. These characteristics are not consistent with fluvial erosion by either precipitation runoff or spring discharge. The gridded valleys are locally wider or more closely spaced, resulting in smaller isolated mesas and more extensive valley surfaces. Progressive degradation and burial of this surface, found in local areas close to the cratered terrain and in large expanses closer to the plains/upland contact to the north, results in broad low-lying plains with small rounded knobs.

2.2.2. Geologic Materials and Age

[20] Little is known about the composition of the transition zone rocks, but the default interpretation (and the most common one) is that the mesas and knobs are equivalent to cratered highland bedrock [e.g., Tanaka et al., 2005]. Alternatively, parts of the old slope of the crustal dichotomy boundary may have been buried to some depth in the Late Noachian Epoch [Irwin et al., 2004]. Geologic mapping based on Mariner 9 and Viking data placed fretted terrains in the cratered plateau or subdued cratered units, respectively, which were interpreted to result from volcanic or aeolian mantling of the heavily cratered units [Lucchitta, 1978; Greeley and Guest, 1978; Scott et al., 1978, 1986–1987; Hiller, 1979]. Guest et al. [1977] noted that fretted terrain in the Cydonia region was restricted to the plateau unit of Mariner 9-based 1:5 M scale geologic maps and suggested

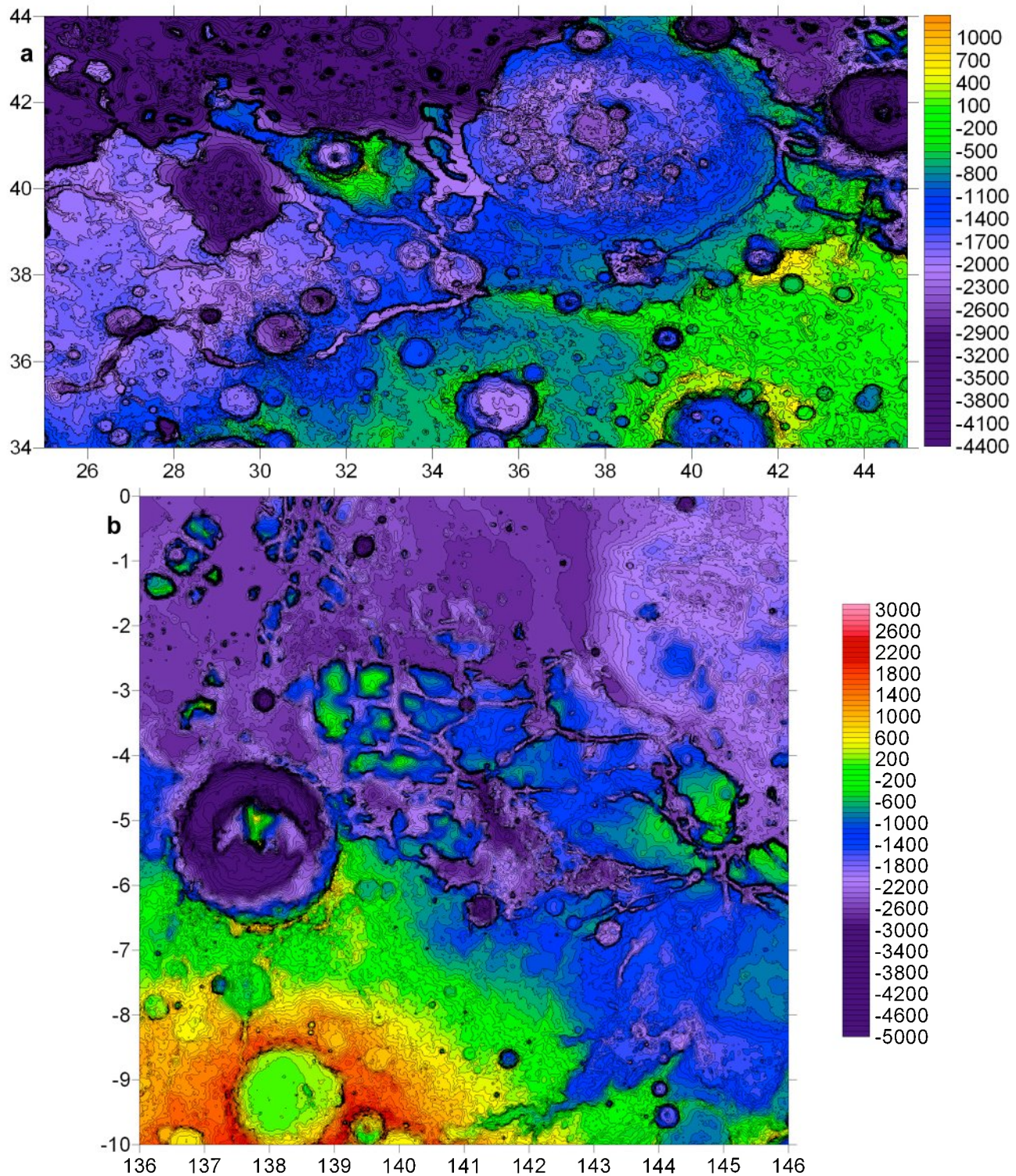


Figure 9. Fretted valleys commonly have an irregular or gridded pattern that was not strongly influenced by surface topography. Note valleys in (a) Deuteronilus Mensae and (b) Aeolis Mensae that are oriented perpendicular to topographic gradients. Both illustrations are MOLA 128 pixel/degree topography with a 100 m contour interval.

that the mesas formed by erosion of this material. Distinguishing features of the cratered plateau or subdued cratered units include: the relative smoothness of its surface at multikilometer through hectometer resolutions (although

considerably more roughness is often seen at meter resolutions), relative to highland intercrater plains; the scarcity of fluvial valleys, and its relatively low crater retention age, particularly at smaller diameters (Figure 10). In the Arabia

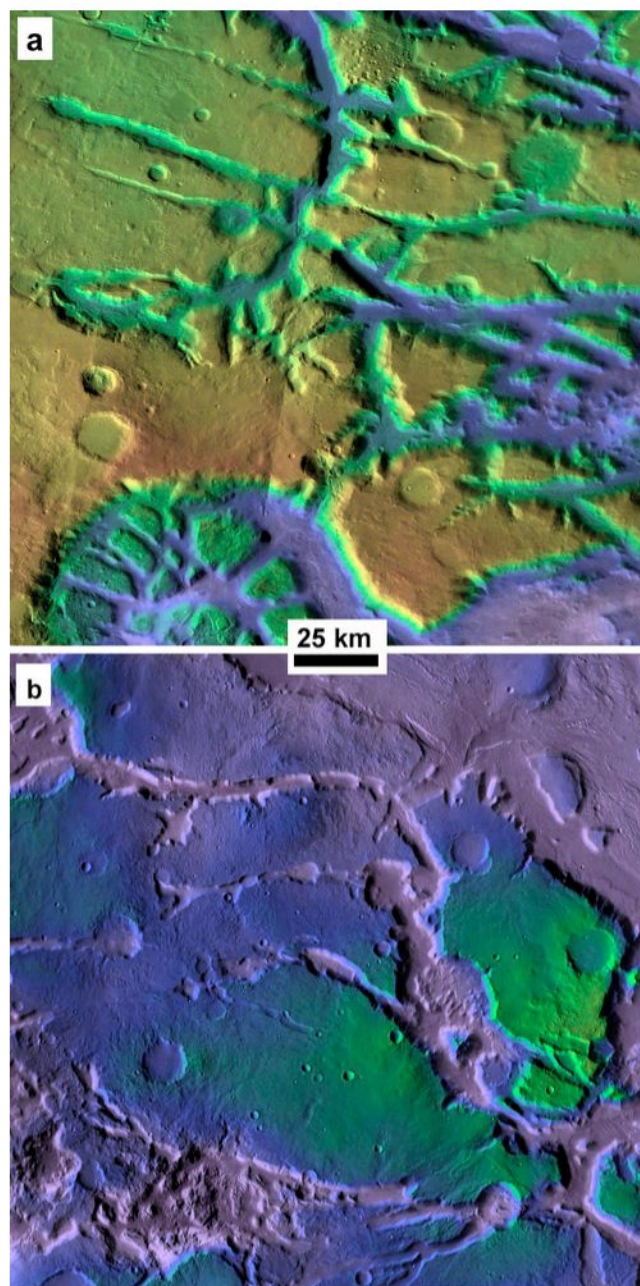


Figure 10. Fretted terrain mesas commonly have smooth or etched surface textures seen at hectometer resolutions, but there is little fluvial dissection of the mesa surfaces or side slopes, suggesting a very limited role for fluvial erosion in development of this landscape. (a) Nilosyrtris Mensae, centered at 31°N, 71°E. (b) Aeolis Mensae, centered at 5°S, 144°E. Images prepared as in Figure 1a.

Terra region that McGill [2000, 2002] mapped at 1:500 K scale, visible crater populations (including degraded or partially buried craters) suggest an Early Noachian age for the cratered highlands surface and a Middle Noachian age for the plateau unit to the north; however, Late Noachian resurfacing reduced the number of smaller craters. Barlow [1990] noted that crater populations vary in knobby terrain but do not exceed the Middle to Late Noachian age of intercrater plains formation in the highlands. This resurfa-

cing history is similar to that determined for Nepenthes Mensae, the transition zone in Amenthes [Frey *et al.*, 1988; Maxwell and McGill, 1988].

[21] Alternative explanations for the relatively smooth plateau unit include later Noachian burial [Scott *et al.*, 1986–1987; Irwin *et al.*, 2004] or erosion to remove its smaller craters [McGill, 2000, 2002]. Erosional landscapes are typically feature-rich, regardless of whether ice, water, wind, mass movement, or impact cratering is the erosional mechanism. Well-developed fluvial landscapes typically have dense drainage networks, clear watershed divides, concave longitudinal grading, and complete integration of the surface area within one or more coherent watersheds. The interpretation that fluvial erosion deeply denuded Arabia Terra [Hynek and Phillips, 2001] is inconsistent with the region's multibasinal, poorly dissected (even by Martian highland standards), and broadly rolling topography [see also Evans *et al.*, 2010]. Grant and Schultz [1990] offered the most satisfactory explanation to date for the Arabia highland surfaces, with some fluvial landscape degradation followed by air fall mantling and limited deflation, which explains the degraded craters as well as the intercrater surfaces with locally poor resistance to wind [see also Fassett and Head, 2007]. Fine-grained, friable materials are much more susceptible to erosion than are competent rocks, particularly in the aeolian regimes of Mars [e.g., Arvidson *et al.*, 1979; Malin and Edgett, 2000; Golombek *et al.*, 2006], and broad areas of the transition zone have aeolian erosional landforms [e.g., Moore, 1990; Irwin *et al.*, 2004; Fassett and Head, 2007]. This characteristic along with a lack of large slump blocks, small flutes in the mesa cap rock created by mass wasting, the low thermal inertia of the plateau, irregularly shaped basins not bounded by fault scarps, and significant erosion of the transition zone after highland crater degradation terminated are all consistent with a mechanically weak material [Irwin *et al.*, 2004]. Mesa talus slopes in Aeolis Mensae have few to no boulders that are visible at meter resolutions [Irwin *et al.*, 2004], but imaging from the High-Resolution Imaging Science Experiment (HiRISE) on Mars Reconnaissance Orbiter shows that boulders up to a few meters in diameter are often concentrated along a discrete layer (Figure 11). The rest of the scarp breaks down quickly to finer-grained materials. Wind-eroded surface materials may not reflect the bulk composition of the transition zone however, and some of the etched surfaces could be relatively thin aeolian mantles of tens to hundreds of meters in thickness [e.g., Fassett and Head, 2007].

[22] In summary, the transition zone may consist of a sequence of fractured highland bedrock, later Noachian volcanic or sedimentary surficial deposits, and younger aeolian mantles that are discontinuously preserved.

2.2.3. Timing of Transition Zone Resurfacing

[23] Geologic mapping and counts of superimposed impact craters have consistently shown an Early Hesperian age for transition zone faulted surfaces, although evolution of that landscape may have begun in the Late Noachian Epoch [Scott *et al.*, 1986–1987; Maxwell and McGill, 1988; Frey *et al.*, 1988; Tanaka *et al.*, 2003, 2005]. Neukum and Hiller [1981] found that the eroded highland surfaces and lowland plains that embay fretted valleys have a similar crater retention age ($N(x)$ = the number of craters greater

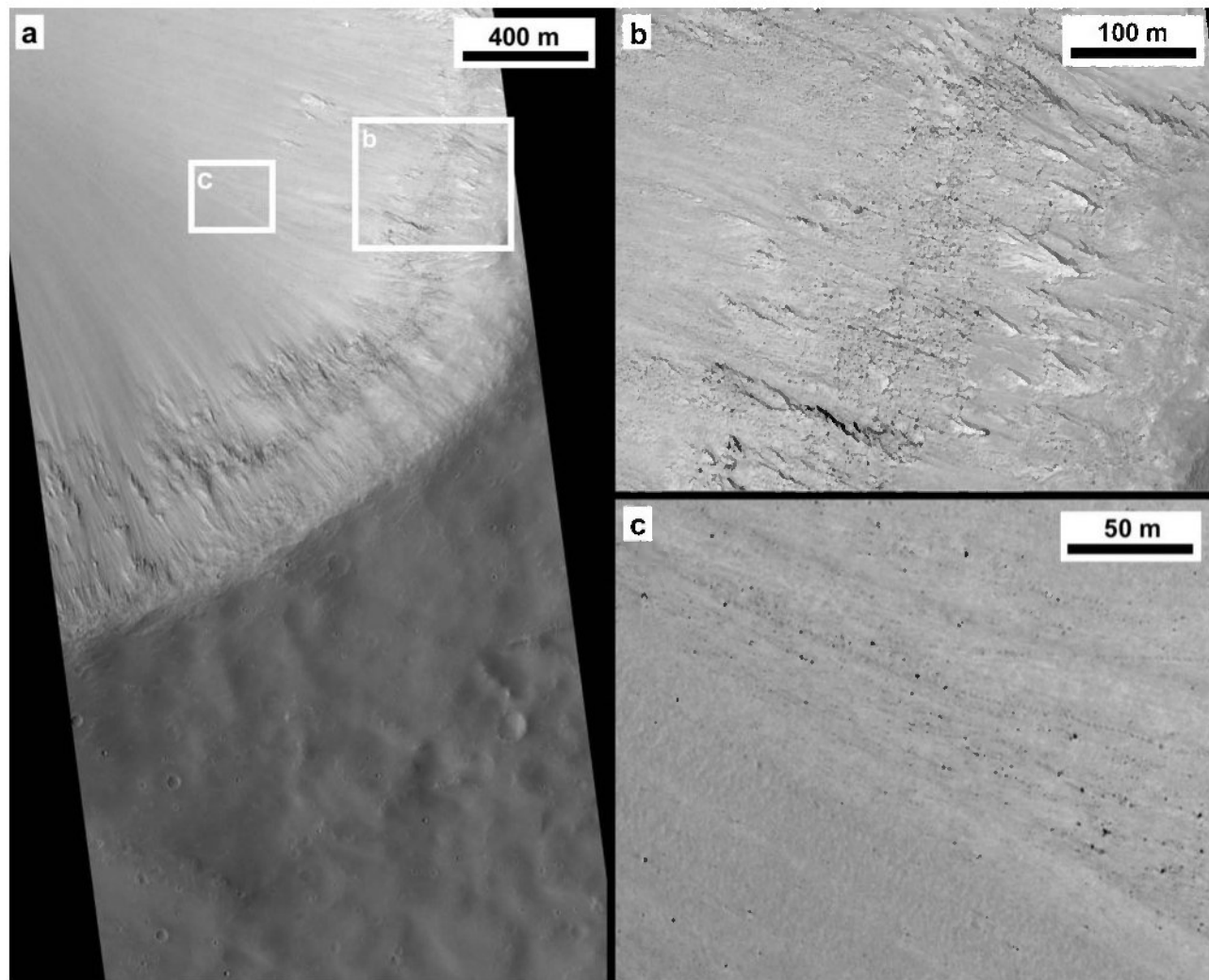


Figure 11. Equatorial fretted terrain in Aeolis Mensae commonly has muted mesa surfaces, easily eroded material exposed on the side slopes, relatively fine-grained talus, and few boulders except in discrete stratigraphic horizons. HiRISE PSP_002451_1770, located at 2.74°S, 132.71°E. Slope is downward to the upper left. (a) Edge of a mesa and stratigraphy exposed near the cap. (b) Enlargement of the boulder-rich horizon and nearby outcrops. (c) Fine-grained talus with few boulders that have rolled downslope from the dark band visible in 11a.

than x km in diameter per 10^6 km²) of $N(1) = 4000$ – $10,000$, or Late Noachian to Early Hesperian in Tanaka's [1986] scheme, and limited the time of formation and erosion to 100–300 Myr. Maxwell and McGill [1988] reached a similar conclusion, finding that faulting along the boundary occurred between $N(5) = 230$ and 190, bracketing the N/H transition at $N(5) = 200$. Fassett and Head [2007] found that aeolian deflation of a Late Noachian mantle in northeastern Arabia Terra occurred with similar timing and speed. Landscape evolution in the transition zone was very rapid relative to erosion of highland valleys and impact craters, forming broad troughs 1–2 km deep when most highland valley networks had incised only tens to hundreds of meters [Goldspiel et al., 1993; Williams and Phillips, 2001; Howard et al., 2005]. Irwin et al. [2004, 2005] observed that Late Noachian valley networks south of Aeolis Mensae were hanging with respect to fretted valleys and had experienced little incision during and after the fretted terrain

development. This relationship suggests that fretted terrain developed much more rapidly than did smaller valley networks or that it formed during a hiatus in highland fluvial activity. Sinuous valleys in northern Arabia Terra are better graded to the troughs of fretted terrain to the north.

[24] The Noachian cratered slope exhibits no relict topography of older fretted terrain, so either cratering and fluvial erosion completely reworked an old fretted landscape in that area, or the geologic processes responsible for fretted terrain were fundamentally unlike those responsible for the cratered slope of the crustal dichotomy boundary. If the same processes were responsible for both surfaces, then some explanation is needed for why they ceased activity and/or shifted to the north during the Noachian Period.

2.2.4. Landscape Evolution in the Transition Zone

[25] Both tectonic and geomorphic modifications are evident in the transition zone, but their origin and relative importance remain poorly understood. It is often difficult to

constrain what fraction of a given valley's volume is attributable to extension or erosion, and the unknown composition of the transition zone rocks complicates identification of reasonable geomorphic processes. Our discussion of how the transition zone may have formed is thus speculative.

[26] The irregularly gridded pattern of valleys (Figures 3, 9, and 10) suggests isotropic extension, perhaps resulting from uplift around the Noachian/Hesperian transition, after fluvial activity had largely declined. Possible causes of this uplift include lower crustal flow, flexure, or volcanic intrusion. Several authors have examined internal heat flows and physical properties of the lower crust that would account for Early Hesperian faulting in the transition zone or preservation of the crustal dichotomy throughout the Pre-Noachian and Noachian Periods [Nimmo, 2005; Guest and Smrekar, 2005; Parmentier and Zuber, 2007], but it is unclear whether both can be achieved without relying on a later input of heat [Nimmo, 2005] or starting the model as late as 4.0 Ga [Guest and Smrekar, 2005]. Flexure associated with Early Hesperian loading of the lowlands may also have affected the transition zone [Watters, 2003a, 2003b]. The ancient cratered slope is not coeval with the Hesperian load, but the fretted terrains are roughly contemporary with lowland plains. It is also possible that pervasive igneous intrusions inflated the crust beneath the transition zone and lowlands during Early Hesperian volcanic resurfacing, potentially accounting for the highly fractured appearance of all Noachian surfaces north of the boundary scarp [Tanaka et al., 1992, 2005], the occurrence of some large enclosed pits in the transition zone (Figure 10) [Baskerville, 1982; Lucchitta, 1984], and the weakness of the remnant crustal magnetism in the lowlands.

[27] Hesperian normal faulting with multikilometer vertical displacements has also been proposed for the transition zone, but this tectonic activity, if it occurred, would be a modification to an older crustal dichotomy boundary rather than its original cause. Smrekar et al. [2004] concluded that the lowland side of the boundary scarp in Protonilus and Nilosyrtris Mensae (Figure 3, parts of the transition zone in Ismenius Lacus and Casius quadrangles, respectively) had been tectonically lowered rather than eroded, based on the need to reconcile two conflicting observations: (1) the 2.5 km of erosion needed to form the boundary scarp would have eliminated the Early Noachian, modified crater population that they observed in the transition zone; however, (2) the boundary scarp is well preserved and crosscuts Middle Noachian plateau materials, requiring extensive tectonic modification of the transition zone in the Middle Noachian or later. Dimitriou [1990] had originally proposed a large normal fault at the plains/upland contact to constrain the minimum volume of material that had been removed from the transition zone between 0°E and 90°E, but he did not present geological or geophysical arguments favoring the fault and lowering of the lowland side, as Smrekar et al. [2004] offered in their study. However, the relief in this complex region attributable to an older crustal dichotomy boundary, Hesperian faulting, or erosion of mantling deposits is not clear.

[28] A dominant role for fluvial erosion in carving fretted valleys and reducing mesas to knobs is unlikely. Unlike rectilinear drainage networks and some of those attributed to

groundwater sapping on Earth, partly due to apparent structural control [Dunne, 1980; Pieri, 1980; Laity and Malin, 1985], there appears to be no preferred orientation of the gridded valleys along hydraulic gradients. In many cases, gridded valleys are oriented perpendicular to local slopes, in contrast with sinuous valleys and branching valley networks (Figures 3 and 9). Continuous downslope flow paths through fretted terrains are rare in both middle and equatorial latitudes, no channels have been observed on the valley floors, and fluvial dissection of the mesa surfaces and scarps is sparse to absent (particularly near the equator), although some sinuous valleys with stubby tributaries debouched into fretted terrain from the highlands [e.g., Carr, 2001].

[29] Debris aprons and lineated valley fills in the midlatitude fretted terrains are attributed to Amazonian ice-facilitated creep and glaciation [e.g., Sharp, 1973; Squyres, 1978; Lucchitta, 1984; Head et al., 2006; Levy et al., 2007]. However, similar features (or degraded remnants of them [e.g., Hauber et al., 2008]) are not found in the more pristine, equatorial fretted terrain of Aeolis and Nepenthes Mensae, and the profiles of nearby degraded craters have not been "softened" by ice as in the midlatitudes [Jankowski and Squyres, 1992, 1993]. Evidence is lacking that glacial movement, mass wasting, or fluvial discharge transported material hundreds of kilometers into the lowlands, although material has been transported away from midlatitude scarps [e.g., Squyres, 1978; Mangold, 2003] and, in some cases, significant distances down confined valleys [Head et al., 2006; Levy et al., 2007]. Moreover, Early Hesperian fretted terrains and Amazonian glacial features are not coeval [e.g., Squyres, 1978; Mangold, 2003; Levy et al., 2007], so ice movement is likely not the main process involved in fretting [Irwin et al., 2004].

[30] Wind has been largely ineffective at modifying basaltic surfaces on Mars, such as Hesperian and younger impact craters and lava flows [Arvidson et al., 1979; Greeley et al., 1982; Craddock and Maxwell, 1993; Craddock et al., 1997; Golombek and Bridges, 2000; Golombek et al., 2006], so its efficacy in parts of the transition zone would depend on a weaker lithology and/or more effective weathering processes and higher atmospheric pressure in the Early Hesperian [e.g., Sharp, 1973; Irwin et al., 2004]. Where materials are more susceptible to it, deflation yields rough surfaces at short wavelengths (e.g., Medusae Fossae [Ward, 1979; Wells and Zimbelman, 1997; Bradley et al., 2002]). For example, in some etched areas of Nilosyrtris Mensae, resistant linear ridges (possible dikes or veins) enclose small basins, presumably indicating tens of meters of deflation [Fassett and Head, 2007]. Pedestal craters and yardangs are found in some areas of Aeolis and Nepenthes Mensae [Irwin et al., 2004], but the large mesas are more resistant than are materials exposed between them, suggesting that the latter may be weaker air fall mantles. Deflation surfaces are common but not ubiquitous in the fretted and knobby terrains, whereas fluvial features are rare to absent. The inverse relationship is found in highland cratered and dissected terrains.

[31] The cause of the decline of geological activity in the transition zone depends largely on knowing what processes were responsible for it. Volcanic resurfacing of the lowlands declined during the Hesperian, before the emplacement of the Vastitas Borealis Formation [Tanaka et al., 2005], and faulting in the transition zone may have been related to this

magmatic activity. Aeolian or fluvial activity would depend on a thicker atmosphere, which is thought to have declined around this time along with rapid weathering processes.

3. Discussion

[32] We find that the crustal dichotomy boundary and transition zone represent two discrete epochs of geological activity that are widely separated in time, and we see no geological record of long-term process continuity between them. This observation does not necessarily rule out some tectonic influence by the crustal dichotomy boundary on fretted terrain, but the latter is not directly associated with the formation of the dichotomy. Here we discuss the implications of these findings on geophysical models of the crustal dichotomy.

3.1. Endogenic and Exogenic Models

[33] We show above that the crustal dichotomy, including the northward-sloping cratered terrain along its margin, formed before the surface cratering record was established. If the traditional model of a declining impact flux is accurate, then the dichotomy developed within a few hundred million years, prior to 4.1–4.33 Ga in Frey's [2006b] scheme. Alternatively, a possible high impact flux in the late heavy bombardment [e.g., Strom *et al.*, 2005; Frey, 2008a] would allow more time (it would also imply a higher Noachian denudation rate than has been calculated previously [Craddock *et al.*, 1997; Golombek *et al.*, 2006]). Even so, scenarios wherein plate tectonics or other long-lived endogenic processes form the crustal dichotomy over ~700–800 Myr [Sleep, 1994; Lenardic *et al.*, 2004] lack the necessary time. Moreover, mountain belts, subduction trenches, volcanoes, faults, and accretional terrains do not occur where plate tectonic models would predict them [Pruis and Tanaka, 1995]. Erosion during and after the Early Noachian Epoch was not adequate to completely remove impact basins of a few hundred kilometers in diameter and a few kilometers in relief, so erosion is not a credible means of erasing comparably sized evidence of plate tectonics, unless it was very early and short-lived.

[34] Convection models for the origin of the dichotomy involve early degree-1 mantle convection with preferential heating, upwelling, and crustal thinning in one hemisphere and downwelling and crustal thickening in the other hemisphere [Zhong and Zuber, 2001; Zuber, 2001; Roberts and Zhong, 2006]. Rapidly developing mantle convection could produce a significant difference in crustal thickness on a time scale of less than 100 Myr [Roberts and Zhong, 2006]. Heterogeneous fractionation of a magma ocean has also been suggested for the early, rapid formation of the crustal dichotomy [Solomon *et al.*, 2005]. An early magma ocean may have caused a gravitationally unstable mantle that could have rapidly overturned, resulting in degree-1 mantle flow and the formation of the crustal dichotomy [Elkins-Tanton *et al.*, 2005].

[35] This study indicates that the Late Noachian to Early Hesperian tectonics associated with the dichotomy boundary are not directly related to its formation or early modification. Tectonic features resulting from the Early to Pre-Noachian formation or modification of the dichotomy boundary are not expected to be preserved. Late-stage modification of the

dichotomy boundary from relaxation or flexure may have been triggered by Late Noachian–Early Hesperian lowlands volcanism [see Watters *et al.*, 2007], including both intrusive and extrusive igneous activity. The degree to which late-stage relaxation or flexure modified the boundary, however, must be less than predicted by existing models [Nimmo, 2005; Guest and Smrekar, 2005; Watters, 2003a, 2003b; Watters and McGovern, 2006]. Moreover, modeling of endogenic causes for Early Hesperian fretted terrain must also be consistent with preservation of the crustal dichotomy throughout the Noachian and perhaps the Pre-Noachian Periods [Parmentier and Zuber, 2007], and it must exclude extensional faulting of the heavily cratered slope in Terra Cimmeria/Sirenum at any time during the visible Noachian cratering record.

[36] Impact hypotheses for the crustal dichotomy [Wilhelms and Squyres, 1984; Frey and Schultz, 1988, 1990; Frey, 2006a, 2006b] maintain that the differences in topography and crustal thickness result from a net redistribution of crust from north to south during one or more large/giant impacts. Most previous reviews have concluded that although multiple large impacts have significantly modified the northern lowlands, they cannot explain the crustal dichotomy without relying on supporting endogenic and/or erosional processes [McGill and Squyres, 1991; Zuber, 2001; Nimmo and Tanaka, 2005; Solomon *et al.*, 2005]. Their arguments rest on several observations. (1) Suitable topographic basins, impact structures, and gravity anomalies are only observed in parts of the lowlands [Smith *et al.*, 1999; Zuber *et al.*, 2000; Neumann *et al.*, 2004] (the need to completely remove both the gravitational and topographic signatures of other putative large impact basins presents a conceptual challenge). Most of the crustal dichotomy boundary lacks the embayments that one would expect from multiple impact basins [McGill and Squyres, 1991]. (2) Unless substantially modified by (or perhaps causing) endogenic processes, overlapping impacts would produce elevated interbasin highlands like those on the Moon rather than a wholesale lowering of a surface [McGill and Squyres, 1991]. (3) There is no topographic or gravitational evidence for thicker crust around the periphery of the lowlands, as would be expected of ejecta from large impacts [McGill and Dimitriou, 1990]. (4) The more large impacts are invoked to form the lowlands, the less statistically probable is their coincidence within the same hemisphere. (5) Frey [2008b] concluded that the Utopia basin formed in prethinned crust, to account for the differences in crustal thickness within highland and lowland basins.

[37] The single giant impact hypothesis is the subject of recent modeling [e.g., Marinova *et al.*, 2008; Nimmo *et al.*, 2008; Andrews-Hanna *et al.*, 2008], and although these studies support a giant impact model, they do not exclude an origin for the crustal dichotomy by mantle convection [Kiefer, 2008]. Relict structures and landforms [Wilhelms and Squyres, 1984] have not been convincingly attributed to a giant impact [McGill and Dimitriou, 1990], but its Pre-Noachian age would make preservation of such features highly unlikely. Modeling suggesting that the crustal dichotomy boundary had an elliptical shape with Tharsis removed [Andrews-Hanna *et al.*, 2008] does not include the thin crust of Arabia Terra. Andrews-Hanna [2010] suggests lower crustal flow following the excavation of the transient

cavity as a means to explain the lower topography and crustal thickness of Arabia Terra. Accounting for the variable transition zone between the highlands and lowlands, including both Arabia Terra and the steep boundary slope in the opposite hemisphere, continues to be an important constraint on future modeling of the crustal dichotomy [see *Watters et al.*, 2007; *Kiefer*, 2008].

3.2. Implications for Future Modeling Efforts

[38] This and other studies provide some general constraints on future modeling efforts.

[39] 1. The crustal dichotomy originated before the preserved Martian cratering record, likely during the Pre-Noachian Period (as used by *Tanaka et al.* [2005]). Geologic constraints do not support long-lived geophysical processes of formation.

[40] 2. Models of the crustal dichotomy should account for both the steep cratered slope from 40°E eastward to 145°W and the lower gradient from 60°W eastward to 40°E. It is unknown whether the steeper and the gentler slopes are original.

[41] 3. Models of the origin of the crustal dichotomy should be constrained by the long-wavelength topography of Noachian cratered terrain. Fractures and faults in the transition zone and lowlands are not coeval with the formation of the crustal dichotomy.

[42] 4. The origin of fretted terrain may be related to the crustal dichotomy in some way, but not to its origin. Any internal process that is invoked to explain fretted terrain should be consistent with preservation of Noachian degraded craters on the highland slope.

4. Conclusions

[43] Features of the crustal dichotomy boundary and transition zone provide important constraints on the age of the crustal dichotomy, and they undermine the utility of Hesperian structures and landforms as ground truth for geophysical models of its formation. Several lines of evidence rule out a Late Noachian to Early Hesperian origin for the crustal dichotomy, slow formative processes that require the entire Noachian Period, and any direct link between the origins of the dichotomy and Early Hesperian fretted/knobby terrains. On the cratered slope along the crustal dichotomy boundary, fresh Hesperian and Amazonian impact craters have rim crests that are inclined subparallel to the slope and interior cavities that are oriented vertically (Figure 6), similar to fresh craters located within the Early Noachian Hellas basin. These features are consistent with impacts on a preexisting slope. Modern topography controlled the flow paths of Late Noachian valley networks, which do not divert from topographic gradients as they would if the dichotomy boundary region had been later tilted (Figure 7). Degraded impact craters have flat to slightly concave, undissected floor deposits, which indicate that no tilting occurred after those deposits were emplaced up to and including the Noachian/Hesperian transition (Figures 1, 2, and 8). In some cases, heavily modified, amphitheater-shaped craters on the slope have flat floors with smaller superimposed craters that were degraded to the cookie cutter rather than amphitheater morphology (Figure 5). This contrast demonstrates that the larger crater

floor was not tilted and reworked after the smaller craters formed in the Middle to Late Noachian Epochs. Normal faults did not cut either visible impact craters or topographically defined impact basins along the top of the cratered slope, suggesting that any flexure of the crustal dichotomy boundary occurred very early (Figures 1 and 2). The age of the cratered slope is consistent with the Early to Pre-Noachian age of the lowland crust suggested by its populations of buried impact craters [*Frey et al.*, 2002; *Frey*, 2006a, 2006b; *Watters et al.*, 2006], remnant crustal magnetism outside of large impact basins [*Connerney et al.*, 2005], and isotopic evidence cited in section 1.

[44] The processes responsible for fretted terrain were short-lived and highly effective relative to Late Noachian crater degradation and valley incision to the south. The localization of Early Hesperian fretted and knobby terrains along the Early to Pre-Noachian crustal dichotomy boundary suggests some kind of connection, but these terrains appear to result from a much later combination of isotropic tensile stress (perhaps due to uplift), related fractures, and erosional processes in some proportion, forming a landscape with no resemblance to the older cratered slope. The relatively smooth surfaces of mesas and the plateau unit in the transition zone likely reflect Noachian erosion and later burial rather than denudation alone. Several features of fretted terrains are not consistent with dominant fluvial erosion, including their irregular valley floor gradients in both middle and equatorial latitudes, typical lack of gullying on mesas, and lack of preferential growth up hydraulic gradients. The formation of fretted terrain resulted in significant base level declines and headward knickpoint propagation for valley networks in northwestern Terra Cimmeria [*Irwin et al.*, 2005], suggesting that large gridded valleys formed much more rapidly than did smaller fluvial valleys in the highlands, or that they represent a hiatus in valley network activity. Glaciation also does not appear to be responsible for fretted terrain. Amazonian debris aprons and lineated valley fills in midlatitude, Hesperian fretted terrain appear to be of glacial origin [e.g., *Squyres*, 1978; *Lucchitta*, 1984; *Head et al.*, 2006; *Levy et al.*, 2007], but these features (or degraded remnants) are not found in contemporary equatorial fretted terrains [*Irwin et al.*, 2004] south of about 20°N–25°N (and they are rare south of 30°N) [*Hauber et al.*, 2008]. Diffusional creep has not modified equatorial impact craters [*Craddock et al.*, 1997; *Forsberg-Taylor et al.*, 2004] as it has many midlatitude craters [*Jankowski and Squyres*, 1992, 1993]. It is possible that the tectonic processes that controlled fretted terrain development were related to lowland volcanic resurfacing and intrusions during the Hesperian Period.

[45] Geological and geophysical observations are thus reconciled around an Early to Pre-Noachian age for the crustal dichotomy. By definition, the Pre-Noachian Period predates the surface cratering record, so constraints by relict landforms on the age of the dichotomy become more equivocal as the age is pushed back toward that time. No impact basins or other surface features are obviously older than the crustal dichotomy, so the maximum time available to form it may be on the order of ~300 Myr in *Frey's* [2006b] scheme, or perhaps more if the late heavy bombardment was a catastrophic spike rather than a gradual decline [e.g., *Strom et al.*, 2005]. Isotopic data referenced in

section 1 may place much tighter constraints on the order of tens of millions of years [Solomon *et al.*, 2005].

[46] Our findings place four constraints on models of the crustal dichotomy: (1) the dichotomy originated before the surface cratering record by a relatively short-lived geological process, (2) both the low-gradient Arabia and the steeper Cimmeria sides of the crustal dichotomy boundary are ancient features of Mars that should be addressed in geophysical modeling studies, (3) long-wavelength Noachian topography rather than smaller Hesperian structures and landforms should be used to constrain modeling, and (4) the formation of fretted and knobby terrains represents a separate geophysical and geomorphic problem that would benefit from detailed modeling and stratigraphic studies. Geological observations may be consistent with a relatively short-lived, very early internal process or a giant impact, but likely not with long-lived plate tectonics, as the cause for lowland formation.

[47] **Acknowledgments.** This study was supported by a Mars Data Analysis Program grant to T. R. Watters. We thank Debra Buczkowski for helpful comments.

References

- Acuña, M. H., *et al.* (1999), Global distribution of crustal magnetization discovered by the Mars Global Surveyor MAG ER Experiment, *Science*, **284**, 790–793.
- Andrews-Hanna, J. C. (2010), Arabia Terra, Mars: A partial ring structure around the Borealis basin and implications for the mechanism of multiring basin formation, *Lunar Planet. Sci. Conf. 41*, Lunar Planet. Inst., Houston, Tex., Abstract 2615.
- Andrews-Hanna, J. C., M. T. Zuber, and W. B. Banerdt (2008), The Borealis basin and the origin of the martian crustal dichotomy, *Nature*, **453**, 1212–1216, doi:10.1038/nature07011.
- Arvidson, R. E. (1974), Morphologic classification of Martian craters and some implications, *Icarus*, **22**, 264–271.
- Arvidson, R. E., E. A. Guinness, and S. Lee (1979), Differential eolian redistribution rates on Mars, *Nature*, **278**, 533–535.
- Bandfield, J. L., V. E. Hamilton, and P. R. Christensen (2000), A global view of Martian surface compositions from MGS-TES, *Science*, **287**, 1626–1630, doi:10.1126/science.287.5458.1626.
- Barlow, N. G. (1990), Constraints on early events in Martian history as derived from the cratering record, *J. Geophys. Res.*, **95**(B9), 14,191–14,201, doi:10.1029/JB095iB09p14191.
- Barlow, N. G. (1995), The degradation of impact craters in Maja Valles and Arabia, Mars, *J. Geophys. Res.*, **100**(E11), 23,307–23,316, doi:10.1029/95JE02492.
- Baskerville, C. A. (1982), Collapse: A mechanism for Martian scarp retreat, in *Reports of the Planetary Geology Program, NASA Tech. Mem. 85127*, pp. 244–252, NASA, Washington, D. C.
- Bhattacharya, J. P., T. H. D. Payenberg, S. D. Lang, and M. C. Bourke (2005), Dynamic river channels suggest a long-lived Noachian crater lake, *Geophys. Res. Lett.*, **32**, L10201, doi:10.1029/2005GL022747.
- Blichert-Toft, J., J. D. Gleason, P. Télouk, and F. Albarède (1999), The Lu–Hf geochemistry of shergottites and the evolution of the Martian mantle–crust system, *Earth Planet. Sci. Lett.*, **173**, 25–39.
- Borg, L. E., L. E. Nyquist, H. Wiesmann, and C.-Y. Shih (1997), Constraints on Martian differentiation processes from Rb–Sr and Sm–Nd isotopic analyses of the basaltic shergottite QUE 94201, *Geochim. Cosmochim. Acta*, **61**, 4915–4931.
- Bradley, B. A., S. E. H. Sakimoto, H. Frey, and J. R. Zimbelman (2002), Medusae Fossae Formation: New perspectives from Mars Global Surveyor, *J. Geophys. Res.*, **107**(E8), 5058, doi:10.1029/2001JE001537.
- Breed, C. S., J. F. McCauley, and M. J. Grolier (1982), Relict drainages, conical hills, and the eolian veneer in southwest Egypt—Applications to Mars, *J. Geophys. Res.*, **87**(B12), 9929–9950, doi:10.1029/JB087iB12p09929.
- Buczkowski, D. L. (2007) Stealth quasi-circular depressions (sQCDs) in the northern lowlands of Mars, *J. Geophys. Res.*, **112**, E09002, doi:10.1029/2006JE002836.
- Buczkowski, D. L., H. V. Frey, J. H. Roark, and G. E. McGill (2005), Buried impact craters: A topographic analysis of quasi-circular depressions, Utopia Basin, Mars, *J. Geophys. Res.*, **110**, E03007, doi:10.1029/2004JE002324.
- Carr, M. H. (1981), *The Surface of Mars*, Yale Univ. Press, New Haven, Conn.
- Carr, M. H. (1995), The Martian drainage system and the origin of valley networks and fretted channels, *J. Geophys. Res.*, **100**(E4), 7479–7508, doi:10.1029/95JE00260.
- Carr, M. H. (2001), Mars Global Surveyor observations of Martian fretted terrain, *J. Geophys. Res.*, **106**(E10), 23,751–23,759, doi:10.1029/2000JE001316.
- Carruthers, M. W., and G. E. McGill (1998), Evidence for igneous activity and implications for the origin of a fretted channel in southern Ismenius Lacus, Mars, *J. Geophys. Res.*, **103**(E13), 31,433–31,444, doi:10.1029/98JE02494.
- Chen, J. H., and G. J. Wasserburg (1986), Formation ages and evolution of Shergotty and its parent planet from U–Th–Pb systematics, *Geochim. Cosmochim. Acta*, **50**, 955–968.
- Chuang, F. C., and D. A. Crown (2005), Surface characteristics and degradation history of debris aprons in the Tempe Terra/Mareotis fossae region of Mars, *Icarus*, **179**, 24–42.
- Connerney, J. E. P., M. H. Acuña, P. J. Wasilewski, N. F. Ness, H. Rème, C. Mazelle, D. Vignes, R. P. Lin, D. L. Mitchell, and P. A. Cloutier (1999), Magnetic lineations in the ancient crust of Mars, *Science*, **284**, 794–798.
- Connerney, J. E. P., M. H. Acuña, N. F. Ness, G. Kletetschka, D. L. Mitchell, R. P. Lin, and H. Rème (2005), Tectonic implications of Mars crustal magnetism, *Proc. Natl. Acad. Sci. U.S.A.*, **102**(42), 14,970–14,975.
- Craddock, R. A., and A. D. Howard (2002), The case for rainfall on a warm, wet early Mars, *J. Geophys. Res.*, **107**(E11), 5111, doi:10.1029/2001JE001505.
- Craddock, R. A., and T. A. Maxwell (1990), Resurfacing of the Martian highlands in the Amenthes and Tyrrhena region, *J. Geophys. Res.*, **95**(B9), 14,265–14,278, doi:10.1029/JB095iB09p14265.
- Craddock, R. A., and T. A. Maxwell (1993), Geomorphic evolution of the Martian highlands through ancient fluvial processes, *J. Geophys. Res.*, **98**(E2), 3453–3468, doi:10.1029/92JE02508.
- Craddock, R. A., T. A. Maxwell, and A. D. Howard (1997), Crater morphometry and modification in the Sinus Sabaeus and Margaritifer Sinus regions of Mars, *J. Geophys. Res.*, **102**(E6), 13,321–13,340, doi:10.1029/97JE01084.
- Davies, G. F., and R. E. Arvidson (1981), Martian thermal history, core segregation, and tectonics, *Icarus*, **45**, 339–346.
- Dimitriou, A. (1990), An estimate of the amount of material removed from the martian fretted terrain, *Geophys. Res. Lett.*, **17**(13), 2461–2464, doi:10.1029/90GL01484.
- Dohrenwend, J. C., A. D. Abrahams, and B. D. Turrin (1987), Drainage development on basaltic lava flows, Cima volcanic field, Southeast California, and Lunar Crater volcanic field, south-central Nevada, *GSA Bull.*, **99**(3), 405–413.
- Dunne, T. (1980), Formation and controls of channel networks, *Prog. Phys. Geogr.*, **4**, 211–239.
- Edgar, L. A., and H. V. Frey (2008), Buried impact basin distribution on Mars: Contributions from crustal thickness data, *Geophys. Res. Lett.*, **35**, L02201, doi:10.1029/2007GL031466.
- Elkins-Tanton, L. T., P. C. Hess, and E. M. Parmentier (2005), Possible formation of ancient crust on Mars through magma ocean processes, *J. Geophys. Res.*, **110**, E12S01, doi:10.1029/2005JE002480.
- Evans, A. J., J. C. Andrews-Hanna, and M. T. Zuber (2010), Geophysical limitations on the erosion history within Arabia Terra, *J. Geophys. Res.*, **115**, E05007, doi:10.1029/2009JE003469.
- Fassett, C. I., and J. W. Head III (2007), Layered mantling deposits in northeast Arabia Terra, Mars: Noachian–Hesperian sedimentation, erosion, and terrain inversion, *J. Geophys. Res.*, **112**, E08002, doi:10.1029/2006JE002875.
- Forsberg-Taylor, N. K., A. D. Howard, and R. A. Craddock (2004), Crater degradation in the Martian highlands: Morphometric analysis of the Sinus Sabaeus region and simulation modeling suggest fluvial processes, *J. Geophys. Res.*, **109**, E05002, doi:10.1029/2004JE002242.
- Frey, H. V. (2006a), Impact constraints on the age and origin of the lowlands of Mars, *Geophys. Res. Lett.*, **33**, L08S02, doi:10.1029/2005GL024484.
- Frey, H. V. (2006b), Impact constraints on, and a chronology for, major events in early Mars history, *J. Geophys. Res.*, **111**, E08S91, doi:10.1029/2005JE002449.
- Frey, H. V. (2008a), Ages of very large impact basins on Mars: Implications for the late heavy bombardment in the inner solar system, *Geophys. Res. Lett.*, **35**, L13203, doi:10.1029/2008GL033515.
- Frey, H. V. (2008b), Mars crustal dichotomy: Large lowland impact basins may have formed in prethinned crust, *Lunar Planet. Sci. Conf. 39*, Lunar Planet. Inst., Houston, Tex., Abstract 1342.

- Frey, H. V., and R. A. Schultz (1988), Large impact basins and the mega-impact origin for the crustal dichotomy on Mars, *Geophys. Res. Lett.*, **15**(3), 229–232, doi:10.1029/GL015i003p00229.
- Frey, H. V., and R. A. Schultz (1990), Speculations on the origin and evolution of the Utopia-Elysium lowlands of Mars, *J. Geophys. Res.*, **95**(B9), 14,203–14,213, doi:10.1029/JB095iB09p14203.
- Frey, H. V., A. M. Semeniuk, J. A. Semeniuk, and S. Tokarcik (1988), A widespread common age resurfacing event in the highland-lowland transition zone in eastern Mars, *Proc. 18th Lunar Planet. Sci. Conf.*, 679–699.
- Frey, H., S. E. Sakimoto, and J. Roark (1998), The MOLA topographic signature at the crustal dichotomy boundary zone on Mars, *Geophys. Res. Lett.*, **25**(24), 4409–4412, doi:10.1029/1998GL900095.
- Frey, H. V., J. H. Roark, K. M. Shockey, E. L. Frey, and S. E. H. Sakimoto (2002), Ancient lowlands on Mars, *Geophys. Res. Lett.*, **29**(10), 1384, doi:10.1029/2001GL013832.
- Goldspiel, J. M., S. W. Squyres, and D. G. Jankowski (1993), Topography of small Martian valleys, *Icarus*, **105**, 479–500.
- Golombek, M. P., and N. T. Bridges (2000), Erosion rates on Mars and implications for climate change: Constraints from the Pathfinder landing site, *J. Geophys. Res.*, **105**, 1841–1854, doi:10.1029/1999JE001043.
- Golombek, M. P., et al. (2006), Erosion rates at the Mars Exploration Rover landing sites and long-term climate change on Mars, *J. Geophys. Res.*, **111**, E12S10, doi:10.1029/2006JE002754.
- Grant, J. A. (1987), The geomorphic evolution of eastern Margaritifer Sinus, Mars, in *Advances in Planetary Geology, NASA Tech. Mem. 89871*, pp. 1–268, NASA, Washington, D. C.
- Grant, J. A., and P. H. Schultz (1990), Gradational epochs on Mars: Evidence from west-northwest of Isidis Basin and Electris, *Icarus*, **84**, 166–195.
- Grant, J. A., and P. H. Schultz (1993), Degradation of selected terrestrial and Martian impact craters, *J. Geophys. Res.*, **98**(E6), 11,025–11,042, doi:10.1029/93JE00121.
- Grant, J. A., C. Koeberl, W. U. Reimold, P. H. Schultz, and D. Brandt (1997), Degradation history of the Roter Kamm impact crater, Namibia, *J. Geophys. Res.*, **102**(E7), 16,327–16,388, doi:10.1029/97JE01315.
- Grant, J. A., et al. (2006), Crater gradation in Gusev crater and Meridiani Planum, Mars, *J. Geophys. Res.*, **111**, E02S08, doi:10.1029/2005JE002465.
- Greeley, R., and J. E. Guest (1978), Geologic map of the Casius quadrangle of Mars, scale 1:500,000, *U. S. Geol. Surv. Misc. Inv. Ser. Map I-1038*, Reston, Va.
- Greeley, R., et al. (1982), Rate of wind abrasion on Mars, *J. Geophys. Res.*, **87**(B12), 10,009–10,024, doi:10.1029/JB087iB12p10009.
- Guest, A., and S. E. Smrekar (2005), Relaxation of the Martian dichotomy boundary: Faulting in the Ismenius Region and constraints on the early evolution of Mars, *J. Geophys. Res.*, **110**, E12S25, doi:10.1029/2005JE002504.
- Guest, J. E., P. S. Butterworth, and R. Greeley (1977), Geological observations in the Cydonia region of Mars from Viking, *J. Geophys. Res.*, **82**, 4111–4120.
- Halliday, A. N., H. Wanke, J.-L. Birck, and R. N. Clayton (2001), The accretion, composition and early differentiation of Mars, *Space Sci. Rev.*, **96**, 197–230.
- Harper, C. L., Jr., L. E. Nyquist, B. Bansal, H. Weismann, and C.-Y. Shih (1995), Rapid accretion and early differentiation of Mars indicated by $^{142}\text{Nd}/^{144}\text{Nd}$ in SNC meteorites, *Science*, **267**, 213–217.
- Hartmann, W. K., and G. Neukum (2001), Cratering chronology and the evolution of Mars, *Space Sci. Rev.*, **96**, 165–194.
- Hauber, E., S. van Gasselt, M. G. Chapman, and G. Neukum (2008), Geomorphic evidence for former lobate debris aprons at low latitudes on Mars: Indicators of the Martian paleoclimate, *J. Geophys. Res.*, **113**, E02007, doi:10.1029/2007JE002897.
- Head, J. W., III, M. A. Kreslavsky, and S. Pratt (2002), Northern lowlands of Mars: Evidence for widespread volcanic flooding and tectonic resurfacing in the Hesperian Period, *J. Geophys. Res.*, **107**(E1), 5003, doi:10.1029/2000JE001445.
- Head, J. W., A. L. Nahm, D. R. Marchant, and G. Neukum (2006), Modification of the dichotomy boundary on Mars by Amazonian midlatitude regional glaciation, *Geophys. Res. Lett.*, **33**, L08S03, doi:10.1029/2005GL024360.
- Hiller, K. H. (1979), Geologic map of the Amenthes quadrangle of Mars, scale 1:5,000,000, *U. S. Geol. Surv. Misc. Inv. Series Map I-1110*, Reston, Va.
- Howard, A. D. (2007), Simulating the development of Martian highland landscapes through the interaction of impact cratering, fluvial erosion, and variable hydrologic forcing, *Geomorphology*, **91**, 332–363, doi:10.1016/j.geomorph.2007.04.017.
- Howard, A. D., J. M. Moore, and R. P. Irwin III (2005), An intense terminal epoch of widespread fluvial activity on early Mars: 1. Valley network incision and associated deposits, *J. Geophys. Res.*, **110**, E12S14, doi:10.1029/2005JE002459.
- Hynek, B. M., and R. J. Phillips (2001), Evidence for extensive denudation of the Martian highlands, *Geology*, **29**, 407–410.
- Irwin, R. P., III, and A. D. Howard (2002), Drainage basin evolution in Noachian Terra Cimmeria, Mars, *J. Geophys. Res.*, **107**(E7), 5056, doi:10.1029/2001JE001818.
- Irwin, R. P., III, T. R. Watters, A. D. Howard, and J. R. Zimbelman (2004), Sedimentary resurfacing and fretted terrain development along the crustal dichotomy boundary, Aeolis Mensae, Mars, *J. Geophys. Res.*, **109**, E09011, doi:10.1029/2004JE002248.
- Irwin, R. P., III, A. D. Howard, R. A. Craddock, and J. M. Moore (2005), An intense terminal epoch of widespread fluvial activity on early Mars: 2. Increased runoff and paleolake development, *J. Geophys. Res.*, **110**, E12S15, doi:10.1029/2005JE002460.
- Jacobsen, S. B. (2005), The Hf-W isotopic system and the origin of the Earth and Moon, *Annu. Rev. Earth Planet. Sci.*, **33**, doi:10.1146/annurev.earth.33.092203.122614.
- Jankowski, D. G., and S. W. Squyres (1992), The topography of impact craters in “softened” terrain on Mars, *Icarus*, **100**, 26–39.
- Jankowski, D. G., and S. W. Squyres (1993), “Softened” impact craters on Mars: Implications for ground ice and the structure of the Martian regolith, *Icarus*, **106**, 365–379.
- Janle, P. (1983), Bouguer gravity profiles across the highland-lowland escarpment on Mars, *Moon Planets*, **28**, 55–67.
- Kochel, R. C., and R. T. Peake (1984), Quantification of waste morphology on Martian fretted terrain, *J. Geophys. Res.*, **89**(S1), C336–C350, doi:10.1029/JB089iS01p0C336.
- Laity, J. E., and M. C. Malin (1985), Sapping processes and the development of theatre-headed valley networks on the Colorado Plateau, *Geol. Soc. Am. Bull.*, **96**, 203–217.
- Lenardic, A., F. Nimmo, and L. Moresi (2004), Growth of the hemispheric dichotomy and the cessation of plate tectonics on Mars, *J. Geophys. Res.*, **109**, E02003, doi:10.1029/2003JE002172.
- Levy, J. S., J. W. Head, and D. R. Marchant (2007), Lineated valley fill and lobate debris apron stratigraphy in Nilosyrtis Mensae, Mars: Evidence for phases of glacial modification of the dichotomy boundary, *J. Geophys. Res.*, **112**, E08004, doi:10.1029/2006JE002852.
- Lillis, R. J., H. V. Frey, and M. Manga (2008), Rapid decrease in Martian crustal magnetization in the Noachian era: Implications for the dynamo and climate of early Mars, *Geophys. Res. Lett.*, **35**, L14203, doi:10.1029/2008GL034338.
- Lingenfelter, R. E., and G. Schubert (1973), Evidence for convection in planetary interiors from first-order topography, *Moon*, **7**, 172–180.
- Lucchitta, B. K. (1978), Geologic map of the Ismenius Lacus quadrangle of Mars, scale 1:5,000,000, *U. S. Geol. Surv. Misc. Inv. Series Map I-1065*, Reston, Va.
- Lucchitta, B. K. (1984), Ice and debris in the fretted terrain, Mars, *J. Geophys. Res.*, **89**(S2), B409–B418, doi:10.1029/JB089iS02p0B409.
- Lucchitta, B. K., H. M. Ferguson, and C. Summers (1986), Sedimentary deposits in the northern lowland plains, Mars, *J. Geophys. Res.*, **91**(B13), E166–E174, doi:10.1029/JB091iB13p0E166.
- Malin, M. C., and K. S. Edgett (2000), Sedimentary rocks of early Mars, *Science*, **290**, 1927–1937.
- Manent, L. S., and F. El-Baz (1986), Comparison of knobs on Mars to isolated hills in eolian, fluvial and glacial environments, *Earth Moon Planets*, **34**, 149–167.
- Mangold, N. (2003), Geomorphic analysis of lobate debris aprons on Mars at Mars Orbiter Camera scale: Evidence for ice sublimation initiated by fractures, *J. Geophys. Res.*, **108**(E4), 8021, doi:10.1029/2002JE001885.
- Marinova, M. M., O. Aharonson, and E. Asphaug (2008), Mega-impact formation of the Mars hemispheric dichotomy, *Nature*, **453**, 1216–1219, doi:10.1038/nature07070.
- Marty, B., and K. Marti (2002), Signatures of early differentiation of Mars, *Earth Planet. Sci. Lett.*, **196**, 251–263.
- Maxwell, T. A., and G. E. McGill (1988), Ages of fracturing and resurfacing in the Amenthes region, Mars, *Proc. Lunar Planet. Sci. Conf.*, **18**, 701–711.
- McCauley, J. F., M. H. Carr, J. A. Cutts, W. K. Hartmann, H. Masursky, D. J. Milton, R. P. Sharp, and D. E. Wilhelms (1972), Preliminary Mariner 9 report on the geology of Mars, *Icarus*, **17**, 289–327.
- McGill, G. E. (2000), Crustal history of north central Arabia Terra, Mars, *J. Geophys. Res.*, **105**(E3), 6945–6959, doi:10.1029/1999JE001175.
- McGill, G. E. (2002), Geologic map transecting the highland/lowland boundary zone, Arabia Terra, Mars: Quadrangles 30332, 35332, 40332, and 45332, *U.S. Geol. Surv. Geol. Invest. Ser. Map I-2746*, Reston, Va.
- McGill, G. E., and A. M. Dimitriou (1990), Origin of the Martian global dichotomy by crustal thinning in the late Noachian or early Hesperian, *J. Geophys. Res.*, **95**(B8), 12,595–12,605, doi:10.1029/JB095iB08p12595.

- McGill, G. E., and S. W. Squyres (1991), Origin of the Martian crustal dichotomy: Evaluating hypotheses, *Icarus*, 93, 386–393.
- McGill, G. E., and D. U. Wise (1972), Regional variations in degradation and density of Martian craters, *J. Geophys. Res.*, 77(14), 2433–2441, doi:10.1029/JB077i014p02433.
- Moore, J. M. (1990), Nature of mantling deposit in the heavily cratered terrain of northeastern Arabia, Mars, *J. Geophys. Res.*, 95(B9), 14,279–14,289, doi:10.1029/JB095iB09p14279.
- Murray, B. C., L. A. Soderblom, R. P. Sharp, and J. A. Cutts (1971), The surface of Mars I. Cratered terrains, *J. Geophys. Res.*, 76(2), 313–330, doi:10.1029/JB076i002p00313.
- Mutch, T. A., R. E. Arvidson, J. W. Head III, K. L. Jones, and R. S. Saunders (1976), *The Geology of Mars*, Princeton Univ. Press, Princeton, NJ.
- Neukum, G., and K. Hiller (1981), Martian ages, *J. Geophys. Res.*, 86(B4), 3097–3121, doi:10.1029/JB086iB04p03097.
- Neumann, G. A., M. T. Zuber, M. A. Wieczorek, P. J. McGovern, F. G. Lemoine, and D. E. Smith (2004), Crustal structure of Mars from gravity and topography, *J. Geophys. Res.*, 109, E08002, doi:10.1029/2004JE002262.
- Nimmo, F. (2005), Tectonic consequences of Martian dichotomy modification by lower-crustal flow and erosion, *Geology*, 33(7), 533–536.
- Nimmo, F., and D. J. Stevenson (2000), Estimates of Martian crustal thickness from viscous relaxation of topography, *J. Geophys. Res.*, 106(E3), 5085–5098, doi:10.1029/2000JE001331.
- Nimmo, F., and K. L. Tanaka (2005), Early crustal evolution of Mars, *Annu. Rev. Earth Planet. Sci.*, 33, 133–161.
- Nimmo, F., S. D. Hart, D. G. Korycansky, and C. B. Agnor (2008), Implications of an impact origin for the Martian hemispheric dichotomy, *Nature*, 453, 1220–1224, doi:10.1038/nature07025.
- Nyquist, L. E., D. D. Bogard, C. Y. Shih, A. Greshake, D. Stoffler, and O. Eugster (2001), Ages and geologic histories of Martian meteorites, *Space Sci. Rev.*, 96, 105–164.
- Parmentier, E. M., and M. T. Zuber (2007), Early evolution of Mars with mantle compositional stratification or hydrothermal crustal cooling, *J. Geophys. Res.*, 112, E02007, doi:10.1029/2005JE002626.
- Phillips, R. J., and R. S. Saunders (1975), The isostatic state of Martian topography, *J. Geophys. Res.*, 80(20), 2893–2898, doi:10.1029/JB080i020p02893.
- Phillips, R. J., R. S. Saunders, and J. E. Conel (1973), Mars: Crustal structure inferred from Bouguer anomalies, *J. Geophys. Res.*, 78(23), 4815–4820, doi:10.1029/JB078i023p04815.
- Phillips, R. J., M. T. Zuber, S. C. Solomon, M. P. Golombek, B. M. Jakosky, W. B. Banerdt, R. M. E. Williams, B. M. Hynek, O. Aharonson, and S. A. Hauck II (2001), Ancient geodynamics and global scale hydrology on Mars, *Science*, 291, 2587–2591.
- Pieri, D. C. (1980), Geomorphology of Martian valleys, in *Advances in Planetary Geology*, NASA Tech. Mem. 81979, pp. 1–160, NASA, Washington, D. C.
- Pruis, M. J., and K. L. Tanaka (1995), The Martian northern plains did not result from plate tectonics, *Lunar Planet. Sci. Conf. 26*, 1147–1148.
- Roberts, J. H., and S. Zhong (2006), Degree-1 convection in the Martian mantle and the origin of the hemispheric dichotomy, *J. Geophys. Res.*, 111, E06013, doi:10.1029/2005JE002668.
- Robinson, C. A. (1995), The crustal dichotomy of Mars, *Earth Moon Planets*, 69, 249–269.
- Schultz, R. A., and H. V. Frey (1990), A new survey of multiring impact basins on Mars, *J. Geophys. Res.*, 95(B9), 14,175–14,189, doi:10.1029/90JB00910.
- Schultz, P. H., R. A. Schultz, and J. Rogers (1982), The structure and evolution of ancient impact basins on Mars, *J. Geophys. Res.*, 87, 9803–9820.
- Scott, D. H. (1978), Mars, highlands-lowlands: Viking contributions to Mariner relative age studies, *Icarus*, 34, 479–485.
- Scott, D. H., E. C. Morris, and M. N. West (1978), Geologic map of the Aeolis quadrangle of Mars, scale 1:5,000,000, U. S. Geol. Surv. Misc. Invest. Ser. Map I-1111, Reston, Va.
- Scott, D. H., K. L. Tanaka, R. Greeley, and J. E. Guest (1986–1987), Geologic maps of Mars, scale 1:1,500,000, U.S. Geol. Surv. Misc. Inv. Ser. Map I-1802, Reston, Va.
- Sharp, R. P. (1968), Surface processes modifying Martian craters, *Icarus*, 8, 472–480.
- Sharp, R. P. (1973), Mars: Fretted and chaotic terrains, *J. Geophys. Res.*, 78(20), 4073–4083, doi:10.1029/JB078i020p04073.
- Sharp, R. P., and M. C. Malin (1975), Channels on Mars, *Geol. Soc. Amer. Bull.*, 86, 593–609.
- Sleep, N. H. (1994), Martian plate tectonics, *J. Geophys. Res.*, 99(E3), 5639–5655, doi:10.1029/94JE00216.
- Smith, D. E., et al. (1999), The global topography of Mars and implications for surface evolution, *Science*, 284, 1495–1503.
- Smith, D. E., et al. (2001), Mars Orbiter Laser Altimeter: Experiment summary after the first year of global mapping of Mars, *J. Geophys. Res.*, 106(E10), 23,689–23,722, doi:10.1029/2000JE001364.
- Smrekar, S. E., G. E. McGill, C. A. Raymond, and A. M. Dimitriou (2004), Geologic evolution of the Martian dichotomy in the Ismenius area of Mars and implications for plains magnetization, *J. Geophys. Res.*, 109, E11002, doi:10.1029/2004JE002260.
- Soderblom, L. A., and D. B. Wenner (1978), Possible H₂O liquid-ice interfaces in the Martian crust, *Icarus*, 34, 622–637.
- Solomon, S., and J. Head (1980), Lunar mascon basins: Lava filling, tectonics, and evolution of the lithosphere, *Rev. Geophys.*, 18(1), 107–141.
- Solomon, S. C., et al. (2005), New perspectives on ancient Mars, *Science*, 307, 1214–1220.
- Squyres, S. W. (1978), Martian fretted terrain: Flow of erosional debris, *Icarus*, 34, 600–613.
- Squyres, S. W. (1979), The distribution of lobate debris aprons and similar flows on Mars, *J. Geophys. Res.*, 84(B14), 8087–8096, doi:10.1029/JB084iB14p08087.
- Strom, R. G., S. K. Croft, and N. D. Barlow (1992), The Martian impact cratering record, in *Mars*, edited by H. H. Kieffer et al., pp. 383–423, Univ. of Arizona Press, Tucson, Ariz.
- Strom, R. G., R. Malhotra, T. Ito, F. Yoshida, and D. A. Kring (2005), The origin of planetary impactors in the inner Solar System, *Science*, 309, 1847–1850.
- Tanaka, K. L. (1986), The stratigraphy of Mars, *J. Geophys. Res.*, 91(B13), E139–E158, doi:10.1029/JB091iB13p0E139.
- Tanaka, K. L., D. H. Scott, and R. Greeley (1992), Global stratigraphy, in *Mars*, edited by H. H. Kieffer et al., pp. 345–382, Univ. of Arizona Press, Tucson, Ariz.
- Tanaka, K. L., J. A. Skinner Jr., T. M. Hare, T. Joyal, and A. Wenker (2003), Resurfacing history of the northern plains of Mars based on geologic mapping of Mars Global Surveyor data, *J. Geophys. Res.*, 108(E4), 8043, doi:10.1029/2002JE001908.
- Tanaka, K. L., J. A. Skinner, and T. M. Hare (2005), Geologic map of the northern plains of Mars, U.S. Geol. Surv. Misc. Invest. Ser. Map I-2888, Reston, Va.
- Terasaki, H., D. C. Rubie, U. Mann, D. J. Frost, and F. Langenhorst (2005), The effects of oxygen, sulfur, and silicon on the dihedral angles between Fe-rich liquid metal and olivine, ringwoodite, and silicate perovskite: Implications for planetary core formation, *Lunar Planet. Sci. Conf. 36*, Lunar Planet. Inst., Houston, Tex., Abstract 1129.
- Ward, A. W. (1979), Yardangs on Mars: Evidence of recent wind erosion, *J. Geophys. Res.*, 84(B14), 8147–8166, doi:10.1029/JB084iB14p08147.
- Warren, P. H. (1985), The magma ocean concept and lunar evolution, *Annu. Rev. Earth Planet. Sci.*, 13, 201–240.
- Watters, T. R. (2003a), Lithospheric flexure and the origin of the dichotomy boundary on Mars, *Geology*, 31, 271–274.
- Watters, T. R. (2003b), Thrust faults along the dichotomy boundary in the Eastern Hemisphere of Mars, *J. Geophys. Res.*, 108(E6), 5054, doi:10.1029/2002JE001934.
- Watters, T. R., and P. J. McGovern (2006), Lithospheric flexure and the evolution of the dichotomy boundary on Mars, *Geophys. Res. Lett.*, 33, L08S05, doi:10.1029/2005GL024325.
- Watters, T. R., C. J. Leuschen, J. J. Plaut, G. Picardi, A. Safaeinili, A. S. M. Clifford, W. M. Farrell, A. B. Ivanov, R. J. Phillips, and E. R. Stofan (2006), MARSIS evidence of buried impact features in the northern lowlands of Mars, *Nature*, 444, 905–908.
- Watters, T. R., P. J. McGovern, and R. P. Irwin III (2007), Hemispheres apart: The crustal dichotomy on Mars, *Annu. Rev. Earth Planet. Sci.*, 35, 621–652.
- Wells, G. L., and J. R. Zimbelman (1997), Extraterrestrial arid surface processes, in *Arid Zone Geomorphology*, edited by D. Thomas, pp. 659–690, John Wiley, New York.
- Wichman, R., and P. Schultz (1989), Sequence and mechanisms of deformation around the Hellas and Isidis impact basins on Mars, *J. Geophys. Res.*, 94(B12), 17,333–17,357, doi:10.1029/JB094iB12p17333.
- Wilhelms, D. E. (1988), Geologic history of the Moon, U.S. Geol. Surv. Prof. Pap. 1348, Reston, Va.
- Wilhelms, D. E., and S. W. Squyres (1984), The Martian hemispheric dichotomy may be due to a giant impact, *Nature*, 309, 138–140.
- Williams, R., and R. Phillips (2001), Morphometric measurements of Martian valley networks from Mars Orbiter Laser Altimeter (MOLA) data, *J. Geophys. Res.*, 106(E10), 23,737–23,751, doi:10.1029/2000JE001409.
- Wise, D. U., M. P. Golombek, and G. E. McGill (1979), Tharsis province of Mars: Geologic sequence, geometry, and a deformation mechanism, *Icarus*, 38, 456–472.
- Zhong, S., and M. T. Zuber (2001), Degree-1 mantle convection and the crustal dichotomy on Mars, *Earth Planet. Sci. Lett.*, 189, 75–84.
- Zuber, M. T. (2001), The crust and mantle of Mars, *Nature*, 412, 220–227.

Zuber, M. T., et al. (2000), Internal structure and early thermal evolution of Mars from Mars Global Surveyor topography and gravity, *Science*, 287, 1788–1793.

T. R. Watters, Center for Earth and Planetary Studies, National Air and Space Museum, Smithsonian Institution, MRC 315, 6th St. and Independence Ave. SW, Washington, DC 20013, USA.

R. P. Irwin III, Planetary Geodynamics Laboratory, NASA Goddard Space Flight Center, Code 698, Greenbelt, MD 20771, USA. (Irwin@psi.edu)